

**DESIGN OF A CONSTANT FORCE COMPLIANT GRIPPER
MECHANISM**

SABİT KUVVETLİ ESNEK KISKAÇ MEKANİZMASI TASARIMI

OĞUZ KAYALI

PROF. DR. ENGİN TANIK
Supervisor

Submitted to
Graduate School of Science and Engineering of Hacettepe University
as a Partial Fulfillment to the Requirements
for the Award of the **Degree of Master of Science**
in **Mechanical Engineering**

2019

ABSTRACT

DESIGN OF A CONSTANT FORCE COMPLIANT GRIPPER MECHANISM

Oğuz KAYALI

Master of Science Thesis

Department of Mechanical Engineering

Supervisor: Prof. Dr. Engin TANIK

December 2019, 65 pages

This thesis combines the knowledge base of the Compliant Mechanism (CM) with the Constant Force Mechanism (CFM) based upon previous works, which initiate and trigger the key principles of design techniques and simplification of the calculation details of the mechanism. The mechanism design techniques are explained and compared with a classical approach, optimization of the designed mechanism will take place with improved performance and range capabilities. The main target is to obtain constant force output range with normal and feasible displacement with a constant force or torque input. The thesis statement namely design of the Constant Force Compliant Gripper Mechanism (CFCGM) is the one of the hot topics in the literature not yet having enough mature invention. The flow charts and iteration procedure of the design techniques and processes are presented. These design techniques begin with classical mechanism design using kinematic analysis and dynamic analysis switching to CM the design and analysis are harder than before which is pointed out in detail in this thesis.

Keywords: Pseudo-rigid-body-model (PRBM), Compliant Mechanism (CM), Constant Force Mechanisms (CFMs), Constant Force Compliant Gripper Mechanism (CFCGM)

ÖZ

Bu tezde tasarlanmak istenilen sabit kuvvetli esnek kısaç mekanizmanın, esnek mekanizmaların benzetim metotları ile klasik bir mekanizmaya benzetimini gerçekleştirerek, klasik mekanizmaların anahtar prensiplerinden de faydalanmak ve hesaplamalarını yapmak ve sonrasında analizlerini yapmak öngörülmektedir. Tasarımda kullanılacak mekanizmada sisteme sabit bir döngüsel moment ya da bir kuvvet ile verilen bir girdi sonrasında çıktı olarak kabul edilebilir bir yer değiştirme ve sabit denilebilecek bir kuvvet çıktısı alınması hedeflenmektedir. Tasarım şartlarına göre tasarlanacak tercihen yekpare aksi durumda kısmen katı bir esnek mekanizma analizlerinde istenilen sonuç alınana kadar değişkenler optimize edilmek sureti ile tekrarlamalı işlemler gerçekleştirilecektir. Klasik mekanizma benzetimlerinde kinematik ve dinamik analizler gerçekleştirilecek sonrasında yapılan hesaplamaları tasarlanan esnek mekanizma yaklaşımları ile elastik ve lineer olmayan davranışların incelenmesi sağlanacaktır. Hesaplamalarda analitik ya da nümerik yapılabirliği kıyaslanacak ve işlemlere devam edilecektir. Esnek mekanizmalarda malzeme seçimi mekanik özellikleri bakımından (dayanım, esneklik, direnç kırılma, vb.) önemlidir. Esnek mekanizma hesaplarında “pseudo-rigid- body-model (PRBM)” yaklaşımlarından faydalanılması planlanmaktadır. Farklı yaklaşımlar ve tasarım teknikleri de bu tezde ayrıca belirtilecektir.

Tez ile hedeflenen sabit kuvvetli esnek kısaç mekanizması olarak temel bir esnek mekanizmanın tasarlanması ve analiz edilmesi, bu suretle temel mekanizma otomotiv, havacılık, biyomekanik, MEMS gibi birçok farklı alanda uygulama alanı bulacaktır.

ACKNOWLEDGEMENTS

This research was triggered by Prof. Dr. Engin TANIK with his tremendous contribution in every pace. He dedicated himself with his all available time to training, guiding and teaching me in both academic and social areas. I acknowledge of him and his wife with all support and giving right directions.

The help and supporting of my managers and company regulations is appreciated and acknowledged.

Most of all, I would like to thank my wonderful wife and my family. She is truly a pillar of strength in my life. I am thankful for her patience with long, odd hours, for her genuine interest in my research, her playful teasing, and her efforts to motivate me through from the beginning to the end with her contribution to make my life well-organized and easier.

TABLE OF CONTENT

ABSTRACT	vii
ÖZ	ix
ACKNOWLEDGEMENTS.....	x
TABLE OF CONTENT	xi
ABBREVIATIONS	xiii
LIST OF TABLES	xiv
LIST OF FIGURES.....	xiv
1 INTRODUCTION AND BACKGROUND	1
1.1 Introduction	1
1.2 Thesis Problem	2
1.3 Background	3
1.3.1 Conventional Mechanism.....	3
1.3.2 Compliant Mechanisms	7
1.3.3 The Pseudo Rigid Body Model (PRBM)	9
1.4 Literature Review	12
2 DESIGN MODEL DEVELOPMENT	13
2.1 Constant Force Mechanism	13
2.1.1 Slider Crank Mechanism.....	13
2.1.2 Variable Stroke Mechanism	14
2.1.3 Virtual Work Approach.....	18
2.1.4 Synthesis.....	20
2.2 Mechanical Properties	32
2.2.1 Material Selection	32
2.2.2 Stress and Force	33
2.3 Optimization.....	35
3 ANALYSIS AND VERIFICATION.....	37
3.1 Introduction of analysis.....	37
3.2 Geometry	39
3.3 Model and Analysis Section	42

3.4	Analysis Preprocessing.....	45
3.5	Results.....	48
4	CONCLUSION.....	53
5	REFERENCES.....	55
6	APPENDIXES.....	57
	Appendix A – Matlab Code.....	57
7	Curriculum Vitae.....	60

ABBREVIATIONS

Table 1 Abbreviations

CAD	Computer Aided Design
CM	Compliant Mechanism
CMFs	Constant Force Mechanisms
CFCGM	Constant Force Compliant Gripper Mechanism
CFD	Computational Fluid Dynamics
DOF	Degree of Freedom
FBD	Free Body Diagram
FM	Flexural Member
MEMS	Micro Electro Mechanical Systems
PRBM	Pseudo Rigid Body Model
RM	Rigid Member
SLFP	Small Length Flexural Pivot

LIST OF TABLES

Table 1 Abbreviations.....	xiii
Table 2 Planar Kinematic Joints Degree of Freedoms	5
Table 3 Ratio of yield strenght to Young's modulus for several materials	33
Table 4 Part number and joint type compliance for Quarter-Geometry	46
Table 5 Tabular Form of MATLAB and ANSYS Results.....	49

LIST OF FIGURES

Figure 1 Example of Compliant Mechanisms [1]	8
Figure 2 Rigid Body Model Approximations [1].....	10
Figure 3 Fixed-free Compliant Beam Conversion to Pseudo Rigid Body Mechanism [5]	11
Figure 4 Small Length Flexural Pivot [5].....	11
Figure 5 Generic Slider Crank Mechanism.....	13
Figure 6 Complaint Slider Crank Mechanism	14
Figure 7 Partially Compliant Variable Stroke Mechanism [4].....	15
Figure 8 Variable Stroke Mechanism Parameters [4]	16
Figure 9 Partial Force Analysis of Variable Stroke Mechanism [4].....	16
Figure 10 Typical load function of the mechanism [4]	20
Figure 11 θ_{13} and θ_{14} with respect to θ_{12}	21
Figure 12 S_{15} with respect to θ_{12}	22
Figure 13 T_{12} with respect to θ_{12}	23
Figure 14 Design procedure of the mechanism according to a given output loading [4]	25

Figure 15 Design chart of the variable stroke mechanism for constant input-load [4]	26
Figure 16 Data selection	27
Figure 17 Data selection	27
Figure 18 Data selection	28
Figure 19 Data selection	29
Figure 20 Pseudo Rigid Body Model	30
Figure 21 Rigid body counterpart of gripper mechanism	31
Figure 22 Rigid Body Replacement	31
Figure 23 Generic Rectangular Beam Cross Section	34
Figure 24 Compliant mechanism based on the PRBM	35
Figure 25 Compliant Mechanism Design Process [5]	36
Figure 26 ANSYS Workbench opening window	38
Figure 27 Opening Engineering Data Assignment	39
Figure 28 Engineering Data Assignment	39
Figure 29 Geometry Section	40
Figure 30 Quarter-Geometry front view in Solid Works 2018	40
Figure 31 ANSYS Geometry Generation	41
Figure 32 Half-body geometry front view in SolidWorks2018	42
Figure 33 Model Section	42
Figure 34 Material Assignments on Parts	43
Figure 35 Joint Type Assignment	43
Figure 36 Mesh analysis of the quarter mechanism	44
Figure 37 Mesh analysis of half mechanism	45
Figure 38 Analysis Inputs	46
Figure 39 Analysis Settings	47
Figure 40 Output Results Selection	48

Figure 41 Equivalent Stress	48
Figure 42 Force creation in X direction on the slider, ANSYS chart	49
Figure 43 Results Comparison - Crank Angle	50
Figure 44 Results Comparison - Slider Displacement	51
Figure 45 Results Comparison - Reaction Force.....	51
Figure 46 Results Comparison	52

1 INTRODUCTION AND BACKGROUND

1.1 Introduction

Compliant mechanism has been arisen due to many advantages such as reduced cost, part count, weight, assembly time and increased sensitivity. A compliant mechanism can be defined as a flexible structure, which uses elastic deformation to achieve force and motion transmission that transfers motion between joints or linkages causing no friction or hysteresis loss. Transmission takes place with amplifying force or motion, changing direction, changing the dynamics or states. There are many products used in life such as wiper, arrow, caps of shampoo, binder clips, paper clips, backpack latch, lids, nail clippers etc. Recent developments takes place in the field of MEMS designing and robotics with variety of units macro, meso, micro, nano. It gains some or all of its motion from the relative flexibility of its members rather than from rigid body joints alone, hence it can often save space, material and assembly labor and maintenance. Wide range of applicable materials is used for application including steel, aluminum, titanium, polymers, glass fibred reinforced polymers, metal-matrix composites shape memory alloys. Elastic materials are mostly used in various CM design and due to the non-linear behavior of the materials engineering calculations and design processes turn into harder. Viscoelastic behavior may cause deviations and axis may drift. Besides of all hard to design and analysis and cannot complete the full rotation when it compared to rigid-link mechanism are disadvantages [1]. As mentioned, one and the most important disadvantages is that it is hard and very complex to design. In order to solve this issue and simplify the analysis, pseudo-rigid-body-model technique (PRBM) or topology optimization have been constantly used in the literature. [1]. In a PRBM technique kinematic update equations and static equilibrium states has to be defined. This technique accurately simulates elastic beams using rigid links and torsion springs, which obey the Hooke's law. Moreover, it enables the simulation of complicated non-linear elastic behaviors using well-established and comparatively simple methods for simulating constrained rigid bodies. The intention is to master and apply the key principles of design to achieve the main target of this thesis, to create preferably a single piece, monolithic or partially compliant mechanism that could be driven and worked to the design specifications. This thesis also covers the design techniques, processes and methods to identify a mechanisms that are suitable for a given

design problem, and relationships and trends between variables. After completion of the mechanism design, analysis and verification of the part are examined in this thesis.

1.2 Thesis Problem

Previous studies have highlighted many problems when designing a constant force producing mechanism and significant effort has been done to resolve these problems. There are some systems that are designed to use complex control loops and algorithms, which results in costly systems and designs. Enlightened with these previous studies and making some correlations in this thesis, CFCGM will be studied with the aim to develop a lower cost mechanism for specific applications.

This work has to be attempted to have enough knowledge about the conventional mechanism design and additionally compliant mechanism and its design approaches. The starting point for this thesis is to undertake sufficient research of constant force mechanism, compliant constant force mechanism, slider crank mechanism and their design techniques and synthesis. Once the research has concluded, the mechanism behavior will be analyzed with respect to stress and force distribution and their transition to a predefined motion. Appropriate measurement of the constant force output of the gripper hands is key to demonstrating success, by having a constant force output range in the entire motion states. This work examines the different points of view; stress distribution of the mechanism, making proper predefined motion, gathering the constant force output from the gripper hands and iterative and harmonized alignment all these aspects. This work outlines a design method that can be used independently of the Pseudo-Rigid-Body-Model (PRBM) in both the technical and theoretical parts.

To support this work, general background information is given in this study, on conventional mechanism basis, compliant mechanism basis and constant force compliant mechanism basis. Additionally, literature reviewed in these areas is referenced. In the next chapter design, review and analysis section is presented together with the behavioral model and development of design.

1.3 Background

1.3.1 Conventional Mechanism

A mechanism is a mechanical device designed to transfer motion, force or energy. A conventional rigid body mechanism usually consists of rigid links connected with one, or more, movable joints. Using such mechanisms many kinds of inputs can be transformed to desired force, motion or energy output. The disadvantages of these mechanisms include friction, wear and heat losses in operation; they also need regular lubrication and maintenance.

Reuleaux defines a mechanism as an 'assemblage of resistant bodies, connected by movable joints, to form a closed kinematic chain with one link fixed and having the purpose of transforming motion'. For any given mechanism, the motion characteristics of its components may be determined by kinematic analysis. The objective is to find the displacements, velocities, accelerations, shock or jerk (second acceleration) of the various members, as well as the paths described and motions performed by certain elements.

In designing a rigid body mechanism kinematic synthesis may be used to create a mechanism to perform a prescribed motion, transfer force or energy to affect the desired output. Kinematic analysis is then used to confirm that the mechanism will perform as expected.

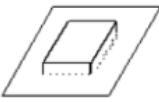
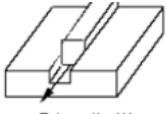
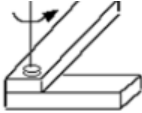



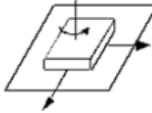
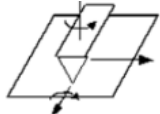
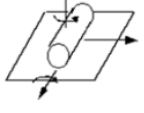
Kinematic Synthesis is broadly divided into two major categories:

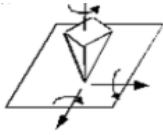

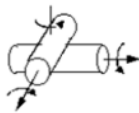
- **Type synthesis:** Given the required performance, decide on what type of mechanism will be suitable. In several applications the most appropriate synthesis will be done using gear trains, linkages, cam mechanisms etc. Another issue arising when constructing the synthesis of a given mechanism is how many links should the mechanism has. The degree of freedom is another important aspect, decide how many separate inputs are connected to the mechanism, hence the required degree of freedom may be determined. After that desired configuration shall be selected before making the first run.
- **Dimensional synthesis:** This determines the significant dimensions and the starting position of a mechanism type for a specified task .The dimensions define the link lengths or pivot-to-pivot distances on binary, ternary(and so on), links,

angle between crank levers, eccentricities, gear ratios, cam-contour dimensions and cam-follower diameters.

A rigid body mechanism is known as conventional mechanism as it includes parts connected with the joints, hinges, sliders, cams, gear joints etc. The degree of freedom is an important feature to determine the motion inputs of the mechanism hence some formulas are commonly used for this purpose. In mechanism design different elements of the mechanism could have different degrees of freedom as depicted in Table 2 Planar Kinematic Joints Degree of Freedoms. This degree of freedom calculation is widely used in robotic applications.

Table 2 Planar Kinematic Joints Degree of Freedoms

Shape Involved	Constraints		Degree of Freedom
	Translators Motion	Rotary Motion	6-# Constraints
Rigid (no motion)  Rigid (no motion)	0	0	0
Prismatic  Prismatic (1)	2	3	1
Revolute  Revolute (1)	3	2	1
Parallel Cylinders  Parallel Cylinders (2)	2	2	2
Cylindrical  Cylindrical (2)	2	2	2
Spherical  Spherical (3)	3	0	3
Planar  Planar (3)	1	2	3
Edge Slider  Edge Slider (4)	1	1	4
Cylindrical Slider  Cylindrical Slider (4)	1	1	4

Shape Involved	Constraints		Degree of Freedom
	Translators Motion	Rotary Motion	6-# Constraints
 Point Slider (5)	1	0	5
 Spherical Slider (5)	1	0	5
 Crossed Cylinders (5)	1	0	5

The equation for Gruebler's formula is given below in order to determine the DOF of plane of the mechanism.

$$F = \lambda * (n - j - 1) + \sum_{i=1}^j f_i$$

or

$$F = \lambda * (n - 1) + \sum_{i=1}^j c_i$$

where

c_i = number of constraints imposed by joints i

f_i = number of DOF permitted by joints i

n = number of links in the mechanism (having one fixed link)

j = number of joints in the mechanism (binary)

λ = number of DOF of a single rigid body in ambient space

F = number of DOF of the whole mechanism

Howell [5] improved this formula and in doing so created one to use in the case of compliant mechanism syntheses as follows.

$$DOF = 6(n_{seg} - 1) - \sum_{j=1}^5 (6 - j)n_{kj} - \sum_{j=1}^5 (6 - j)n_{cj} - 6n_{fix} + \sum_{j=1}^6 j n_{scj}$$

n_{seg} = number of segments (rigid or compliant)

n_{kj} = number of kinematic pairs allowing j relative DOF

n_{cj} = number of elastic pairs allowing j relative DOF

n_{fix} = number of fixed connections

n_{scj} = number of segments with segment compliance of j

1.3.2 Compliant Mechanisms

A compliant mechanism is a flexible mechanism, which has highly elastic behavior under load when compared to rigid bodies. There are many factors affecting mechanism flexibility, such as material properties and geometry. Unlike rigid link mechanisms, compliant mechanisms achieve at least some mobility from the deflection of the flexible members as opposed to the conventional movable connector joints. Deflection on the other hand depends on stiffness and stress distribution as well as the strength of the construction material. In a compliant mechanism analysis, usually the required deflection is known, and the force necessary to produce the deflection and stress must be calculated. In this study, a model will be designed and analyzed in sections with stress and force feasibilities. There are many kinds of compliant mechanism used in real life as given in Figure 1 [1]. Other important properties are the noise and vibration characteristics of the compliant mechanism, normally these are much less or even zero noise and vibration when compared to conventional mechanism.

Compliant mechanisms may be manufactured on different scales from macro, meso, micro, nano scales or even bigger. Motion is achieved without hinges, joints or sliders. Elastic members drive mobility and this result in a smooth transition of motion. The design stages are difficult because besides managing the motion, the forces, torques or energy absorption are important characteristics.

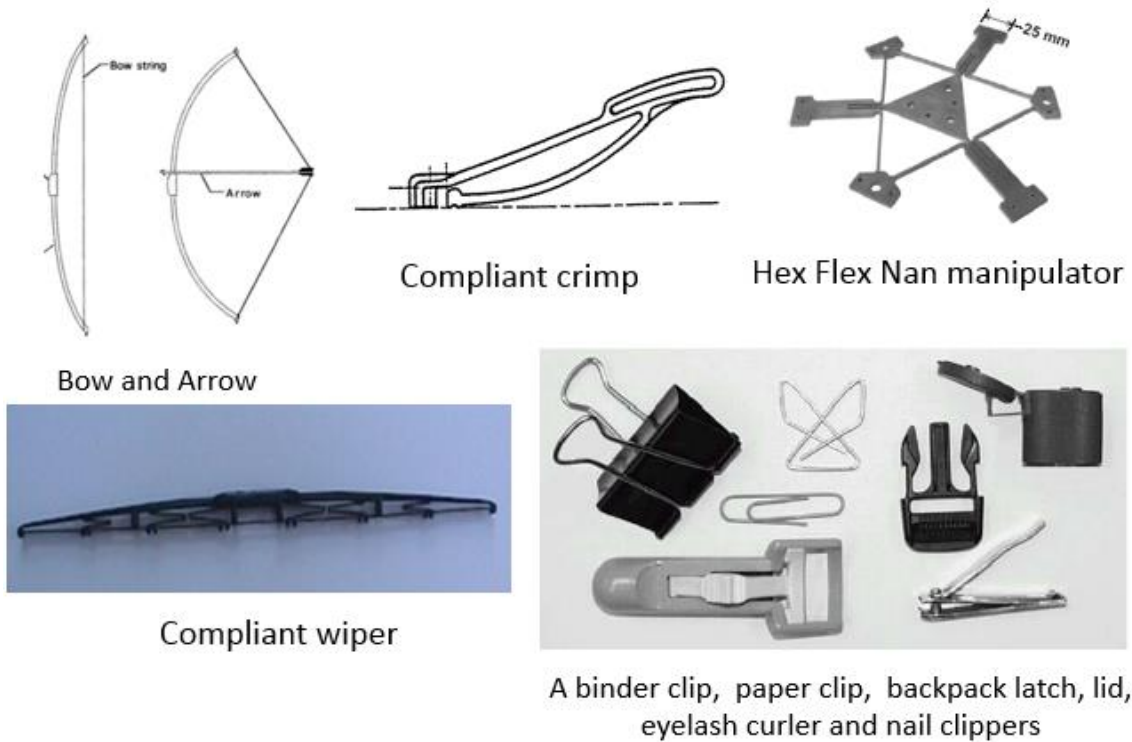


Figure 1 Example of Compliant Mechanisms [1]

1.3.3 The Pseudo Rigid Body Model (PRBM)

The main reason why the PRBM has to be used in any given design solution is that it ensures a reasonable method for systems subjected to large and nonlinear deflection. Because it is such an important design technique, the PRBM approach is used in order to model the system and/or system elements deflection of flexible members with rigid body equivalents and force characteristics. After this design step has been completed, rigid link theories maybe used to analyze the compliant mechanism.

Within this tremendous innovation to model adaptation, PRBM builds a bridge that connects rigid body mechanism theory with compliant mechanism theory. In any specific design objectives, the PRBM approach has great effectiveness and efficiencies on a trial and error analysis. It has the advantage for the designer that prototyping any mechanism is more convenient than numerical analysis. In addition to that, it offers a chance to perform system analysis in nonlinear finite element analysis, and then prototype and test the system.

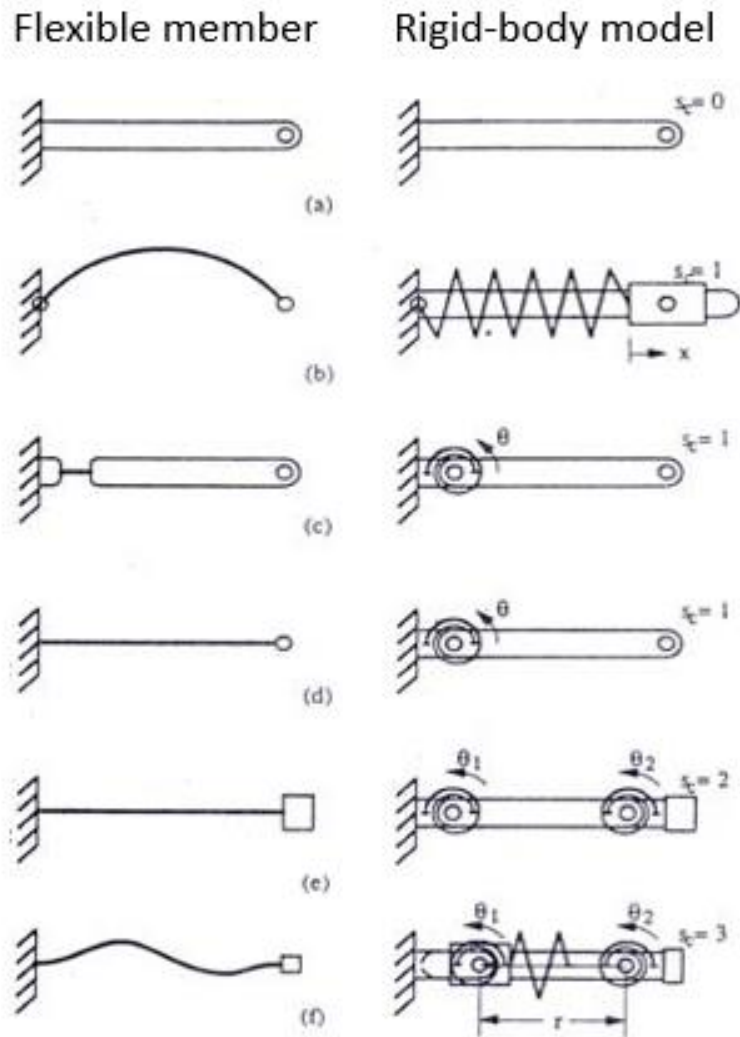


Figure 2 Rigid Body Model Approximations [1]

In kinematics or a rigid body approach, compliant segments are illustrated as several rigid links connected together by pin joints, torsion springs are added to resist torsion as shown in the Figure 2. The value of spring constants and where to place it in the model, are calculated differently depending on types of segments.

The conversion of a cantilever compliant beam with force at free end, in some cases called fixed-free compliant beam, into a rigid body approximation is calculated as shown in Figure 3. The solution to the fixed-free compliant beam could be done either analytically or numerically.

Fixed-free compliant beam

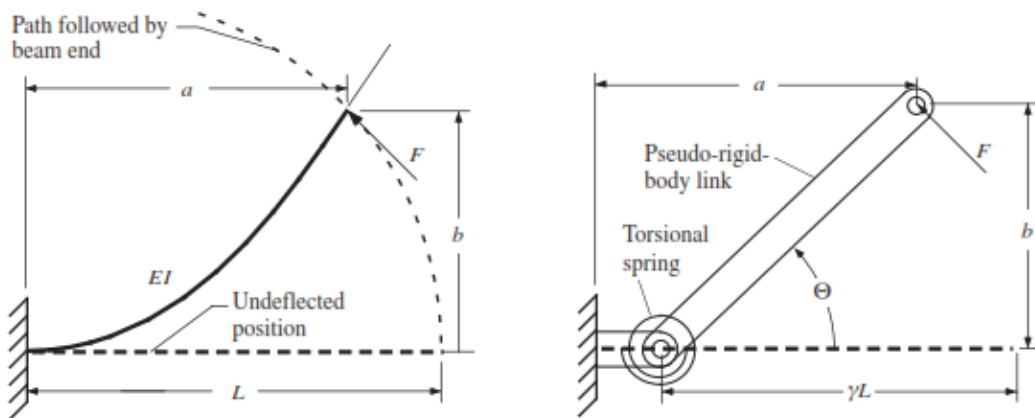


Figure 3 Fixed-free Compliant Beam Conversion to Pseudo Rigid Body Mechanism [5]

Another widely used technique is “Small length flexural pivot”. The main difference from fixed the free compliant beam is that there is a much shorter flexible section than the rigid section and hence the motion of the system could be modeled as two rigid segments combined with a pin joint which is called “characteristic pivot” at the center of the flexible section. It is clearly shown in the Figure 4 at the location of the torsional spring. This approximation works only if the flexible segment is much smaller than the rigid section. In this method the actual material of the part is elastic but the longer section behaves as if it was rigid under deflection.

Small length flexural pivot

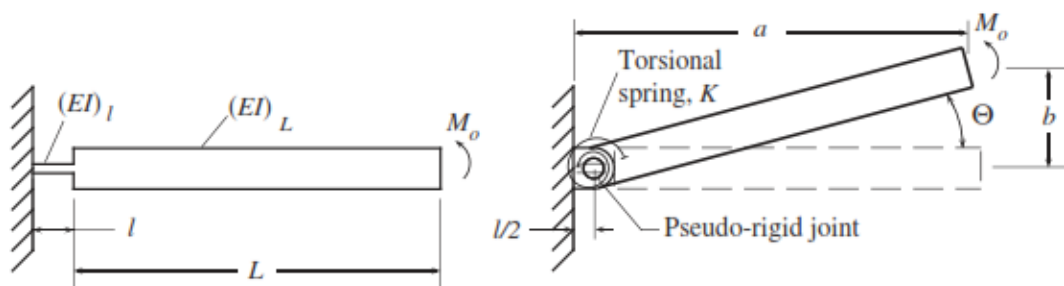


Figure 4 Small Length Flexural Pivot [5]

In Figure 4, the cantilever beam includes two segments, the short one is flexible and the longer one behaves as if it were rigid despite being made from elastic material. The reason for it, the length of the rigid part is much longer than the flexible segment ($L \gg l$) more than 10 times at least.

1.4 Literature Review

In literature there are some important studies relating to a constant force application, which it can be assumed starts with the development of a constant-force tension springs, known as “Neg’ator”, which consists of a coil of flat spring material that has been created using a heavy forming operation. When unstressed, the material tends to form a tight coil. These springs exhibit little change in load with deflection (Wahl, 1963)[8]. In addition, would have been used in creating constant-torque spring motors, which are capable of producing 50 revolutions on one wind. (Wahl, 1963)[8]. Much work has also been done to develop drive units that produce a constant force. These include electrical, hydraulic, and pneumatic systems (Nathan, 1985) [7]. As part of this method, a robot was used to keep a constant normal force on a surface. In other work (Chang and Fu, 1997)[2], a complex deburring model was used to produce a drive system that maintained a constant normal force on the work piece while following a prescribed path. Successful drive systems have been developed and demonstrated. Adapting these systems in terms of size and geometry a variable height application of the compliant constant force robot end-effectors has been developed (Chao-Chieh Lan and Jhe-Hong Wang, Yi-Ho Chen, 2010)[3]. In a compliant model analysis to design a compliant variable stroke mechanism output load function includes some constant force ranges (Tanik and Söylemez, 2010)[4]. Recently, layered design of a compliant mechanism structure solution has been studied to handle various size of objects within the constant force outputs. In this study, an experimental set up has been used to prove; the design objectives, the layered design objectives and that the end constant force output range has been achieved. Load cell disturbance distances are constraints of this study (Jung-Yuan Wang, Chao-Chieh Lan, 2014)[6]. A small scale application of a constant force compliant gripper mechanism based on a buckled-fixed guided-beam was studied. In this particular case results demonstrate a constant force output range was obtained with negligible errors in both force and displacement outputs (Yilin Liu and Qingsong Xu*, 2016)[9].

2 DESIGN MODEL DEVELOPMENT

2.1 Constant Force Mechanism

2.1.1 Slider Crank Mechanism

A slider-crank mechanism converts translational motion to rotary motion or vice versa. The reciprocating piston that is used in internal combustion engines is a well-known application of the slider crank mechanism. A slider crank mechanism possesses four links and four joints. These are; fixed link, crank, coupler link (connecting rod) and slider connected with three revolute and one prismatic joints. The stroke is defined as total displacement of the slider between the two extreme positions, the dead centers. A generic sketch for the slider crank given in the Figure 5.

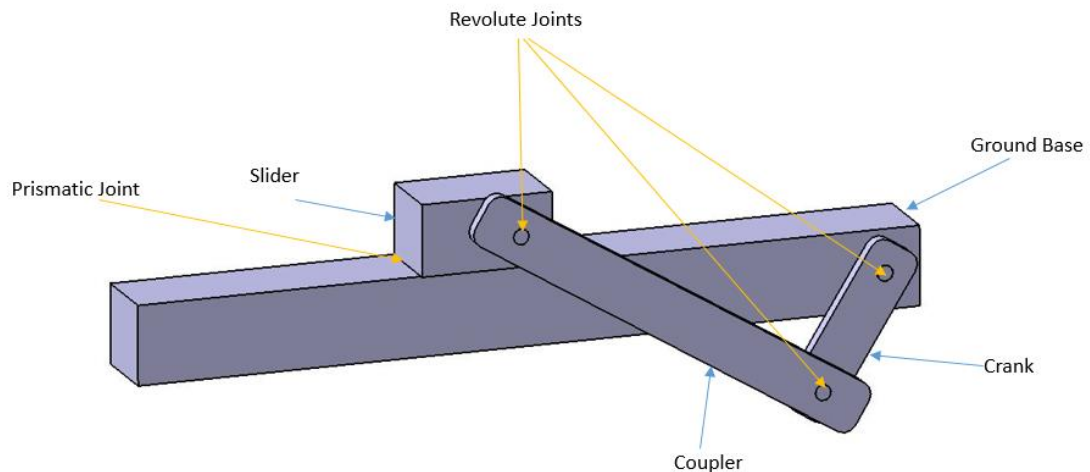


Figure 5 Generic Slider Crank Mechanism

A compliant slider crank mechanism is presented in Figure 6. There are several differences between compliant and conventional, rigid, slider crank mechanisms. Due to the flexible hinges, analysis and design of compliant mechanisms are more complex and harder to calculate. Instead of the revolute joints flexible segments known as small-length flexural pivots (SLFP) are used. Due to the flexural stiffness of these segments, torsional springs are added to the Pseudo Rigid Body Model (PRBM) as shown in Figure 6. In the literature, researchers analyze compliant mechanisms with PRBM. Due to the short length

of the flexible segments with respect to the rigid part, flexural pivots act as kinematic pairs as shown in Figure 6.

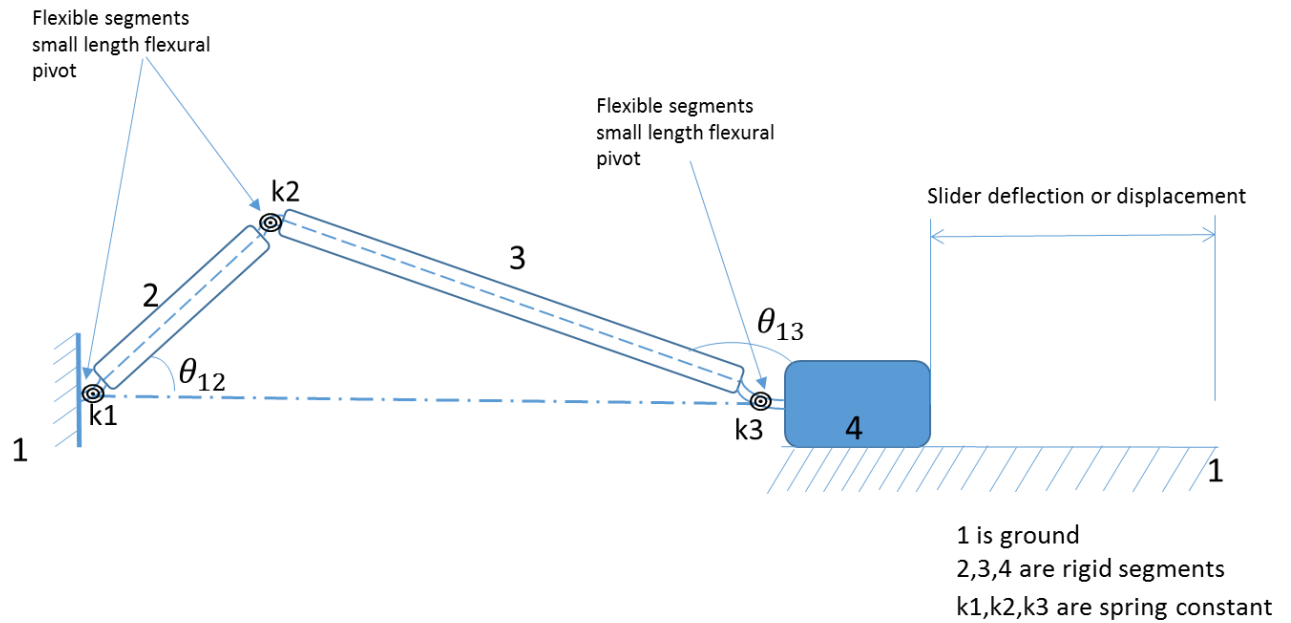


Figure 6 Compliant Slider Crank Mechanism

2.1.2 Variable Stroke Mechanism

In order to obtain a constant force for long stroke, an under actuated slider crank mechanism is chosen for this study [4]. The partially compliant variable stroke mechanism is presented in Figure 7. During the design and analysis stages, SLFPs are modeled as torsional springs and flexible links considering their thickness and proper length. Figure 7, section (a), (b) and (c) are adapted from [4].

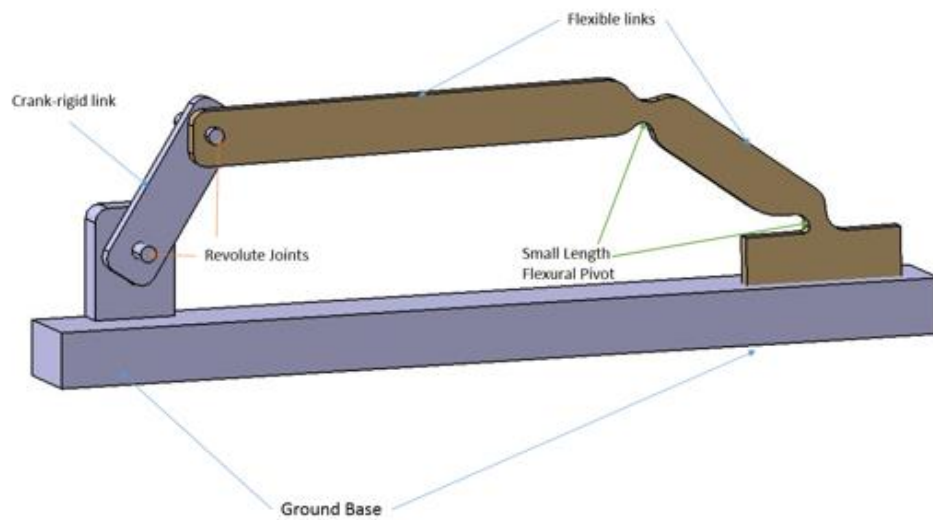
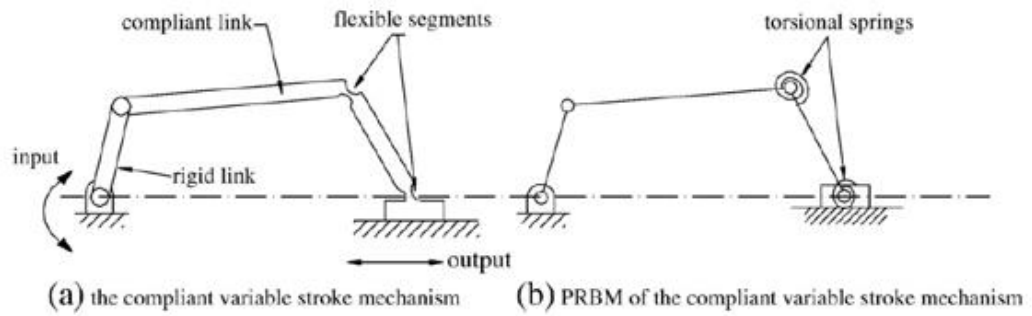


Figure 7 Partially Compliant Variable Stroke Mechanism [4]

For the analysis of this mechanism the method of virtual work is used. The torque input is at link 2 (rigid link). S_{min} indicates minimum the S_{max} indicates the maximum stroke of the slider. Displacement of the slider is in between these two values and given in the sketch as S_{15} .

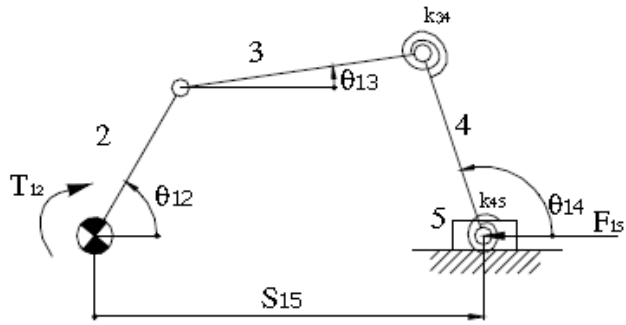


Figure 8 Variable Stroke Mechanism Parameters [4]

Positions and link numbers are given in the sketch. There are also flexible segments which are shown in the FBD as torsional spring effects for convenience on Figure 8 and Figure 9 [4].

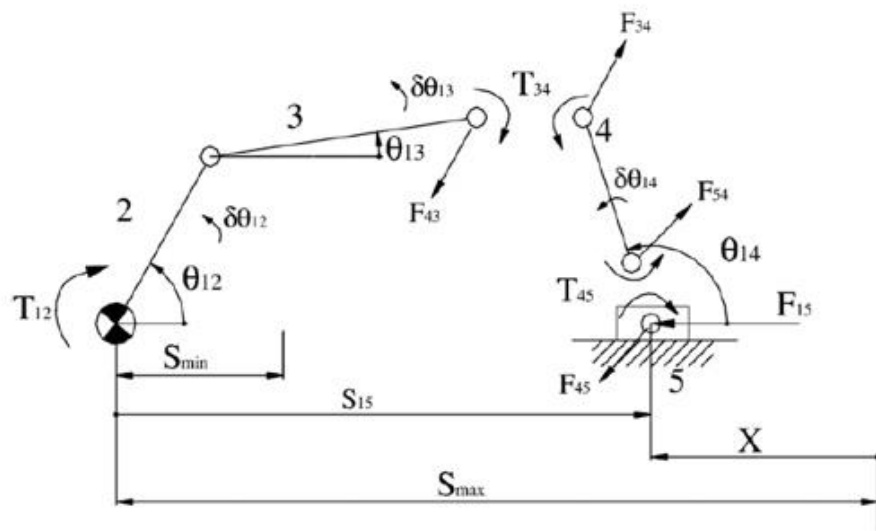
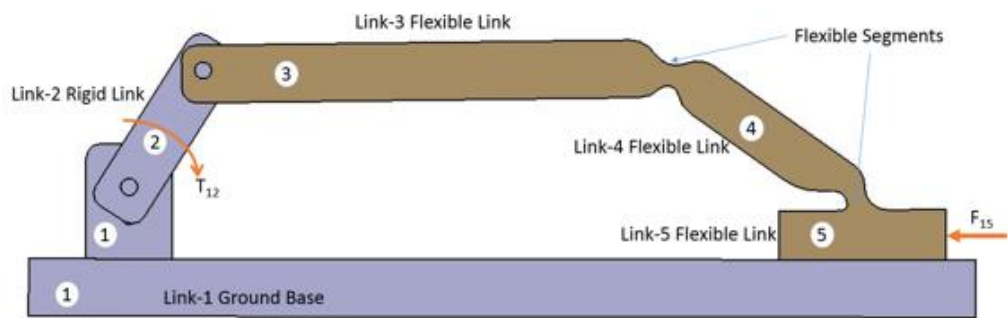


Figure 9 Partial Force Analysis of Variable Stroke Mechanism [4]

Beginning the related mathematical calculation for this system starting with the loop closure equations, the link lengths are a_2, a_3, a_4 .

$$a_2 * \cos \theta_{12} + a_3 * \cos \theta_{13} - a_4 * \cos \theta_{14} = S_{15} \quad (1)$$

$$a_2 * \sin \theta_{12} + a_3 * \sin \theta_{13} - a_4 * \sin \theta_{14} = 0 \quad (2)$$

Differentiating Equations (1) and (2);

$$-a_2 * \sin \theta_{12} \partial \theta_{12} + a_3 * \sin \theta_{13} \partial \theta_{13} - a_4 * \sin \theta_{14} \partial \theta_{14} = \partial S_{15} \quad (3)$$

$$a_2 * \cos \theta_{12} \partial \theta_{12} + a_3 * \cos \theta_{13} \partial \theta_{13} - a_4 * \cos \theta_{14} \partial \theta_{14} = 0 \quad (4)$$

make the related trigonometric and mathematical calculation; multiplying equation 3 with $\cos \theta_{14}$ and Equation 4 with $\sin \theta_{14}$ and then summing them is equal to the following;

$$\begin{aligned} a_3 * (\sin \theta_{14} * \cos \theta_{13} - \cos \theta_{14} * \sin \theta_{13}) \partial \theta_{13} \\ = a_2 * (\sin \theta_{12} * \cos \theta_{14} - \cos \theta_{12} * \sin \theta_{14}) \partial \theta_{12} + \cos \theta_{14} \partial S_{15} \end{aligned}$$

then;

$$\partial \theta_{13} = \frac{a_2 * \sin (\theta_{12} - \theta_{14}) \partial \theta_{12} + \cos \theta_{14} \partial S_{15}}{a_3 * \sin (\theta_{14} - \theta_{13})} \quad (5)$$

multiplying equation 3 with $\cos \theta_{13}$ and equation 4 with $\sin \theta_{13}$ and then summing them is equal to the following;

$$\begin{aligned} a_2 * (\sin \theta_{12} * \cos \theta_{13} - \cos \theta_{12} * \sin \theta_{13}) \partial \theta_{12} + \cos \theta_{13} \partial S_{15} \\ = a_4 * (\sin \theta_{14} * \cos \theta_{13} - \cos \theta_{14} * \sin \theta_{13}) \partial \theta_{14} \end{aligned}$$

then;

$$\partial \theta_{14} = \frac{a_2 * \sin (\theta_{12} - \theta_{13}) \partial \theta_{12} + \cos \theta_{13} \partial S_{15}}{a_4 * \sin (\theta_{14} - \theta_{13})} \quad (6)$$

Now, we provided that, Equations (1-6) are exactly as same as in Tanik's study [4].

2.1.3 Virtual Work Approach

Virtual work is the work done by a real force acting through a virtual displacement or a virtual force acting through a real displacement. Virtual displacement is any displacement consistent with the constraints of the structure, such as satisfying the boundary conditions at supports. A virtual force is any system of forces in equilibrium. In the variable stroke mechanism given in Figure 9, all internal forces and virtual displacements on it are depicted. Kinematic and static force analyses of the variable stroke mechanism are performed. It is assumed that masses of the links are negligible and operating speeds are slow in this stage. Therefore, the entire analysis is based on the static equilibrium. For the analysis of the multi degree-of-freedom mechanisms the method of virtual work will be used.

If T_{12} and F_{15} are the external forces, then;

$$\partial W_1 = -T_{12} \partial \theta_{12} \quad (7)$$

$$\partial W_2 = -F_{15} \partial S_{15} \quad (8)$$

PRBM torsional spring effect as an internal;

$$\partial W_3 = -T_{34} \partial \theta_{13} + T_{34} \partial \theta_{14} \quad (9)$$

$$\partial W_4 = T_{45} \partial \theta_{14} \quad (10)$$

$$T_{34} = k_{34} * (\theta_{13} - \theta_{14} + c_{34}) \quad (11)$$

$$T_{45} = k_{45} * (-\theta_{14} + c_{45}) \quad (12)$$

Where k_{34} and k_{45} are linear spring stiffness; c_{34} and c_{45} are the spring initial position constants which are related to the angle between the connected links as specified before.

Applying the virtual work principles to the system,

$$\partial W = \partial W_1 + \partial W_2 + \partial W_3 + \partial W_4$$

$$\partial W = -T_{12} \partial \theta_{12} - F_{15} \partial S_{15} + T_{34} (\partial \theta_{14} - \partial \theta_{13}) + T_{45} \partial \theta_{14} \quad (13)$$

Substituting (5) and (6) to the equation (13)

$$\begin{aligned}
\partial W = & -T_{12}\partial\theta_{12} - F_{15}\partial S_{15} \\
& + T_{34} \left(\frac{a_2 * \sin (\theta_{12} - \theta_{13})\partial\theta_{12} + \cos \theta_{13}\partial S_{15}}{a_4 * \sin (\theta_{14} - \theta_{13})} \right. \\
& \left. - \frac{a_2 * \sin (\theta_{12} - \theta_{14})\partial\theta_{12} + \cos \theta_{14}\partial S_{15}}{a_3 * \sin (\theta_{14} - \theta_{13})} \right) \\
& + T_{45} \left(\frac{a_2 * \sin (\theta_{12} - \theta_{13}) \partial\theta_{12} + \cos \theta_{13}\partial S_{15}}{a_4 * \sin (\theta_{14} - \theta_{13})} \right)
\end{aligned}$$

then the equation yields

$$\begin{aligned}
\partial W = \partial\theta_{12} \left(-T_{12} + \frac{T_{34} * a_2 * \sin (\theta_{12} - \theta_{13})}{a_4 * \sin (\theta_{14} - \theta_{13})} - \frac{T_{34} * a_2 * \sin (\theta_{12} - \theta_{14})}{a_3 * \sin (\theta_{14} - \theta_{13})} \right. \\
\left. + \frac{T_{45} * a_2 * \sin (\theta_{12} - \theta_{13})}{a_4 * \sin (\theta_{14} - \theta_{13})} \right) + \partial S_{15} \left(-F_{15} + \frac{T_{34} * \cos \theta_{13}}{a_4 * \sin (\theta_{14} - \theta_{13})} \right. \\
\left. - \frac{T_{34} * \cos \theta_{14}}{a_3 * \sin (\theta_{14} - \theta_{13})} + \frac{T_{45} * \cos \theta_{13}}{a_4 * \sin (\theta_{14} - \theta_{13})} \right) \\
\partial W = \partial\theta_{12}\phi_1 + \partial S_{15}\phi_2
\end{aligned}$$

Where

$$\begin{aligned}
\phi_1 = & -T_{12} + \frac{T_{34} * a_2 * \sin (\theta_{12} - \theta_{13})}{a_4 * \sin (\theta_{14} - \theta_{13})} - \frac{T_{34} * a_2 * \sin (\theta_{12} - \theta_{14})}{a_3 * \sin (\theta_{14} - \theta_{13})} \\
& + \frac{T_{45} * a_2 * \sin (\theta_{12} - \theta_{13})}{a_4 * \sin (\theta_{14} - \theta_{13})} \\
\phi_2 = & -F_{15} + \frac{T_{34} * \cos \theta_{13}}{a_4 * \sin (\theta_{14} - \theta_{13})} - \frac{T_{34} * \cos \theta_{14}}{a_3 * \sin (\theta_{14} - \theta_{13})} + \frac{T_{45} * \cos \theta_{13}}{a_4 * \sin (\theta_{14} - \theta_{13})}
\end{aligned}$$

in applying the virtual work principles $\phi_1 = \phi_2 = 0$

then,

$$T_{12} = k_{34} * (\theta_{13} - \theta_{14} + c_{34}) * \left(\frac{a_2 * \sin (\theta_{12} - \theta_{13})}{a_4 * \sin (\theta_{14} - \theta_{13})} - \frac{a_2 * \sin (\theta_{12} - \theta_{14})}{a_3 * \sin (\theta_{14} - \theta_{13})} \right) + k_{45} * (-\theta_{14} + c_{45}) * \left(\frac{a_2 * \sin (\theta_{12} - \theta_{13})}{a_4 * \sin (\theta_{14} - \theta_{13})} \right) \quad (14)$$

$$F_{15} = k_{34} * (\theta_{13} - \theta_{14} + c_{34}) * \left(\frac{\cos \theta_{13}}{a_4 * \sin (\theta_{14} - \theta_{13})} - \frac{\cos \theta_{14}}{a_3 * \sin (\theta_{14} - \theta_{13})} \right) + k_{45} * (-\theta_{14} + c_{45}) * \left(\frac{\cos \theta_{13}}{a_4 * \sin (\theta_{14} - \theta_{13})} \right) \quad (15)$$

2.1.4 Synthesis

Synthesis of the mechanism will include several successive iterations to find out the close approximation. First to understand the mechanism behavior take the lengths of the links 2 and 4 to be a unit length, take the spring stiffness to be $k_{34} = k_{45} = k = 100 \text{ Nmm/rad}$, the initial position constants to be $c_{34} = c_{45} = 2.618 \text{ rad}$ and the initial force load to be 200N. A typical load function of the mechanism is given in Figure 10.

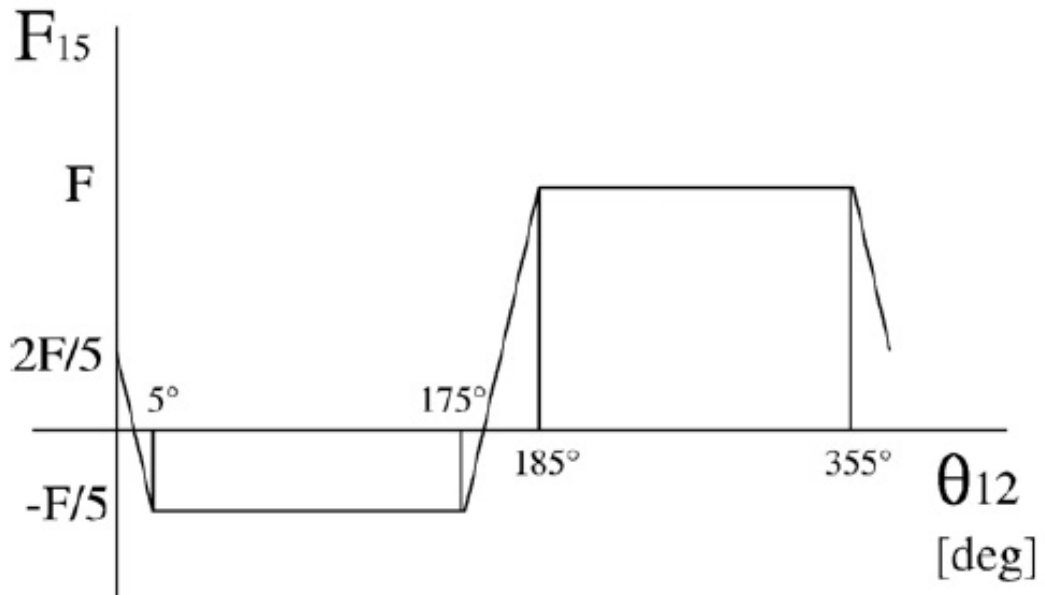


Figure 10 Typical load function of the mechanism [4]

The unknown parameters θ_{13} , θ_{14} , S_{15} , T_{12} remain hence equation (1), (2), (14), (15) could be solved simultaneously to determine and understand the behavior of the system. 4 unknown and 4 nonlinear equations could not be solved analytically but solved numerically.

There are some methods which could be used to solve these equations, such as Newton Raphson method using the partial equations but the *fsolve* function of Matlab is preferred to generate a proper solution in order to prevent unstable behavior. The code is designed to use previous solution responses in every step. The same set of initial estimates for the zero degree of crank angle may not be appropriate for another crank angle. Therefore, in

order to obtain a proper solution quickly, the code used for the solution is modified so that initial estimates are obtained from the previous cycle's set of solutions.

The code is given in Appendix-A, and the behavior of these parameters are depicted in Figure 11, Figure 12, Figure 13. θ_{14} is obtained in the range of 150 degree to 115 degree and is nearly constant.

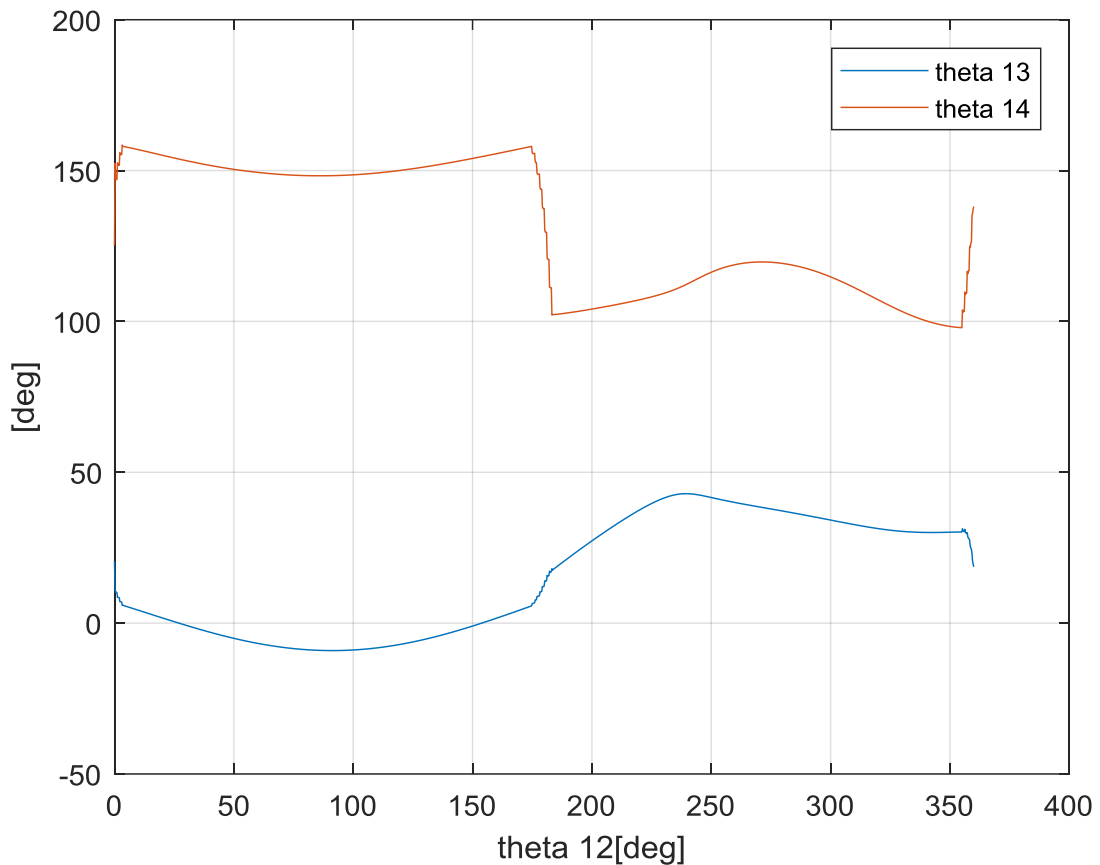


Figure 11 θ_{13} and θ_{14} with respect to θ_{12}

In obtaining these graphs, the virtual work principle is used to generate all virtual displacements, active (external) forces and generalized forces assuming a generalized equilibrium state. If an identical mechanism is in equilibrium, the virtual work of all active forces disappear in each step of virtual displacement and the state of the generalized equilibrium is assured as an identical mechanical system with all active forces vanishing, related calculations have been done in previous sections. In the particular case the unconstrained mechanism is analyzed, with additional work it could be converted to use

cases in different configurations. Because of the under actuated multi degree of freedom mechanism, working zone of the output link is not defined. Additionally the output link oscillation interval depends on the output load magnitude and parameters. In this case for resistive loads, when $\theta_{12}=0$ and $\theta_{12}= 180^\circ$ the mechanism is approximately on the dead centers.

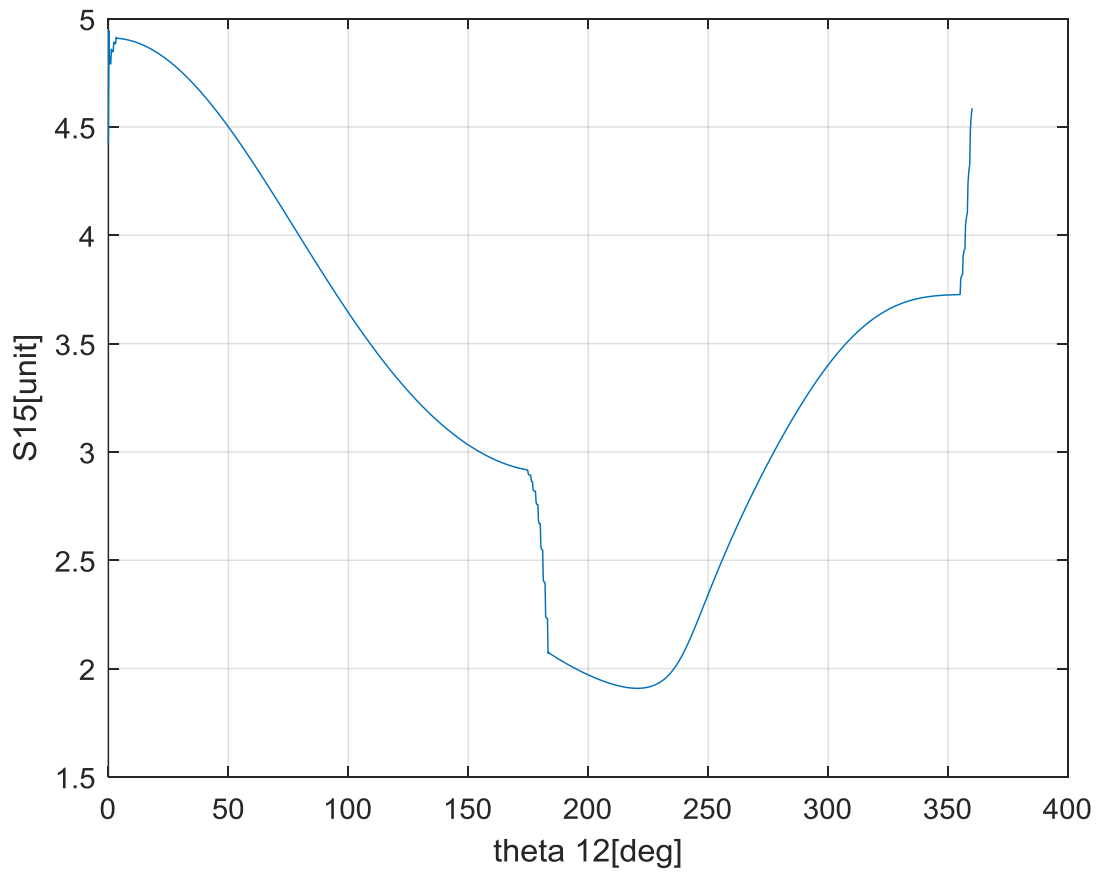


Figure 12 S_{15} with respect to θ_{12}

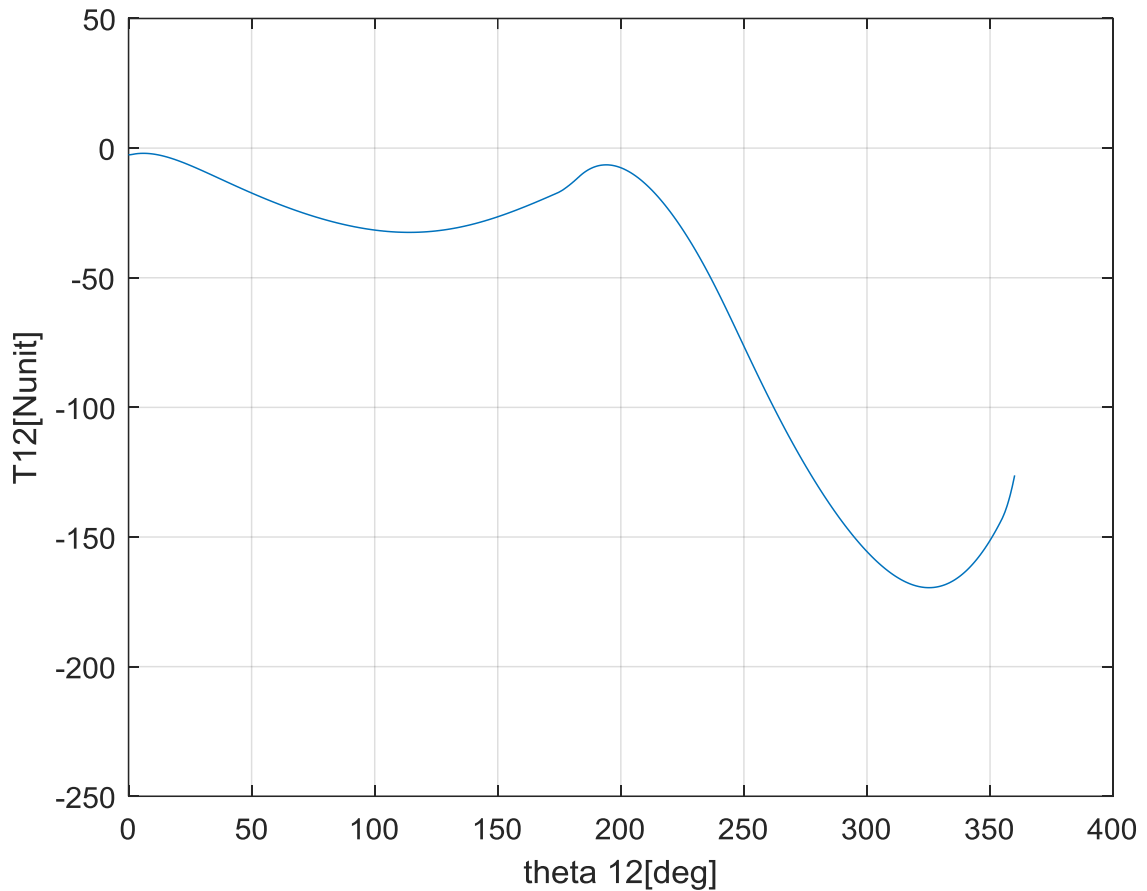


Figure 13 T_{12} with respect to θ_{12}

There are seven separate structure parameters defined in the mechanism as given, these are a_2 , a_3 , a_4 , k_{34} , k_{45} , c_{34} , and c_{45} . In order to obtain an understandable design chart, the number of free parameters has to be reduced. In this under-actuated mechanism output, the loading force function is dependent on the kinematics of the mechanism.

There are different approaches to the construction of the design charts, for instance the mechanism design charts of the variable stroke mechanism with respect to a given output loading is the one way, another one is to construct design charts of the variable stroke mechanism with respect to a given constant input torque after generalization of the parameters. Hence starting with the generalization of the parameters is the first step.

Initially, all related equations can be divided by or multiplied with a_2 or k_{ij} to obtain dimensionless link proportions. In addition, the force and spring constants can be simplified. Spring constant and output force can be considered as a single design parameter. Dividing equations (14) and (15) by k_{34} , more useful ratios can be obtained, $F_{15} \cdot a_2 / k_{34}$ and T_{12} / k_{34} . In addition, for simplification the spring initial position constants can

be the same ($c_{34}=c_{45}=c$) during the design procedure. In order to generalize the approach, the unit length can be taken into consideration. Therefore, the unit of spring constants becomes N-unit/rad.

Dividing equation (1) and (2) by a_2

$$\cos \theta_{12} + \frac{a_3}{a_2} * \cos \theta_{13} - \frac{a_4}{a_2} * \cos \theta_{14} = \frac{S_{15}}{a_2} \quad (16)$$

$$\sin \theta_{12} + \frac{a_3}{a_2} * \sin \theta_{13} - \frac{a_4}{a_2} * \sin \theta_{14} = 0 \quad (17)$$

Dividing equation (14) by k_{34} and multiplying equation (15) with a_2/k_{34} ;

$$\frac{T_{12}}{k_{34}} = (\theta_{13} - \theta_{14} + c_{34}) * \left(\frac{a_2 * \sin(\theta_{12} - \theta_{13})}{a_4 * \sin(\theta_{14} - \theta_{13})} - \frac{a_2 * \sin(\theta_{12} - \theta_{14})}{a_3 * \sin(\theta_{14} - \theta_{13})} \right) + \frac{k_{45}}{k_{34}} * (-\theta_{14} + c_{45}) * \left(\frac{a_2 * \sin(\theta_{12} - \theta_{13})}{a_4 * \sin(\theta_{14} - \theta_{13})} \right) \quad (18)$$

$$\frac{F_{15} * a_2}{k_{34}} = (\theta_{13} - \theta_{14} + c_{34}) * \left(\frac{\cos \theta_{13}}{\frac{a_4}{a_2} * \sin(\theta_{14} - \theta_{13})} - \frac{\cos \theta_{14}}{\frac{a_3}{a_2} * \sin(\theta_{14} - \theta_{13})} \right) + \frac{k_{45}}{k_{34}} * (-\theta_{14} + c_{45}) * \left(\frac{\cos \theta_{13}}{\frac{a_4}{a_2} * \sin(\theta_{14} - \theta_{13})} \right) \quad (19)$$

Then finally Equation (16), (17), (18), (19) have some design parameters such as, a_3/a_2 , a_4/a_2 , k_{45}/k_{34} and $\frac{F_{15} * a_2}{k_{34}}$ or $\frac{T_{12}}{k_{34}}$. In order to obtain the design chart these parameters have to be used.

The variable stroke compliant mechanism is a system where the input torque is constant (assuming an actuator applying constant torque to the crank of the mechanism). This kind of mechanism can be useful for grasping various shapes and sizes of objects according to output force characteristics. A design chart can be constructed for given input torque and structure parameters defined in earlier paragraphs. This chart includes the output-loading force corresponding to link proportions and stroke. However, the stroke interval is unknown at the beginning and for arbitrarily selected values of the stroke; it may not be possible to solve the equation of motion of the mechanism. Hence some assumptions have to be made to change the value of a_4/a_2 , keeping constant $c_{34}=c_{45}=c$ and a_3/a_2 , finally defining $F_{15}=0$ then equation (16), (17), (18), (19) could be solved numerically with *using cubic spline interpolation* to interpolate the data and the full rotation cycle. Then, S_{max}/a_2

and S_{min}/a_2 are determined. In the next step for the same a_4/a_2 value the numerical solution takes place with $S_{15}/a_2 = \{S_{min}/a_2 \text{ to } 0.8S_{max}/a_2\}$ for a set of T_{12}/k . The root of the nonlinear equations cannot be determined for the given input torque. Therefore, a method to determine the stroke interval of the mechanism is required. Design procedure could be used defined in the Figure 14 [4]. Applying the design procedure, a design chart is obtained as depicted in Figure 15 [4]. The important thing is that the parameters in the axes in Figure 15 are dimensionless and in the design state some points on this graph will be selected and the design will be based on this approach with a trial and error, iterative process.

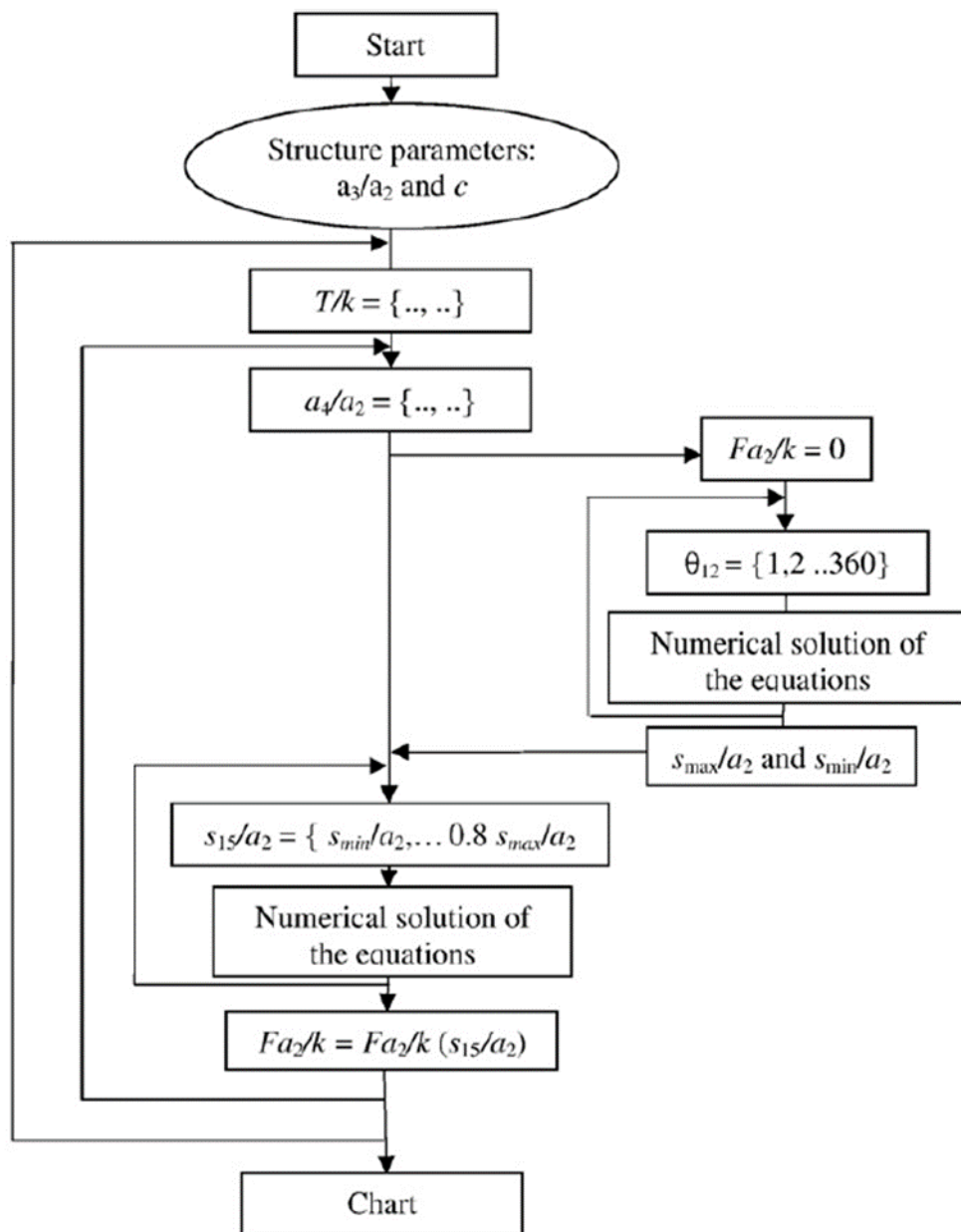


Figure 14 Design procedure of the mechanism according to a given output loading [4]

In this design chart, for one of the axes, a new parameter X is used rather than S_{15} ($X=S_{\max}-S_{15}$). With this parameter, the chart represents the general spring characteristics of the mechanism using Matlab (Appendix A) –. At the first step, $S_{15}=S_{\max}$ is obtained when $F_{15}=0$; hence, $X=0$ ($S_{15}=S_{\max}$) for $F_{15}=0$.

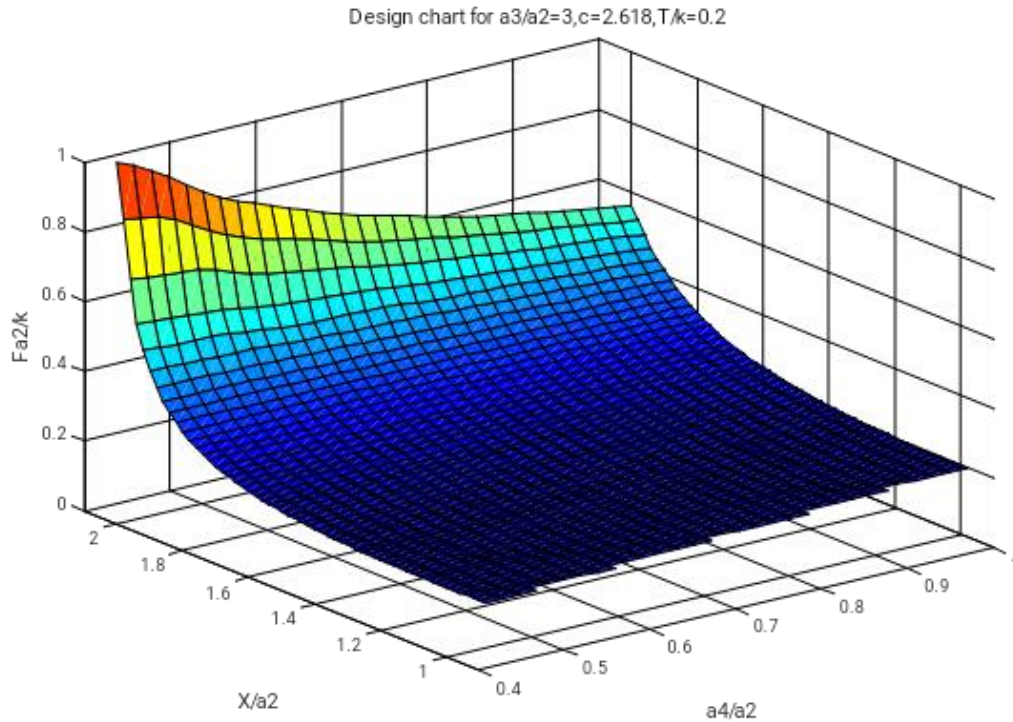


Figure 15 Design chart of the variable stroke mechanism for constant input-load [4]

2.1.4.1 Parameters and Constraints Selection

In the parameters and constraint selection section, the design chart constant force section (flat region on the graph) is focused on and some selected point's data (end points of the data region) will be analyzed. As mentioned before $X=S_{\max}-S_{15}$, the ΔX value is important to the design. Let us point out the selected points values as given below;

Figure 16 and Figure 17;

$$\frac{a_4}{a_2} = 0.6 \rightarrow \frac{X}{a_2} = 0.92 \text{ to } \frac{X}{a_2} = 1.56$$

$$\frac{F * a_2}{k} = \sim 0.2 \text{ to } \frac{F * a_2}{k} = \sim 0.24$$

Hence $\frac{\Delta X}{a_2} = 0.64$

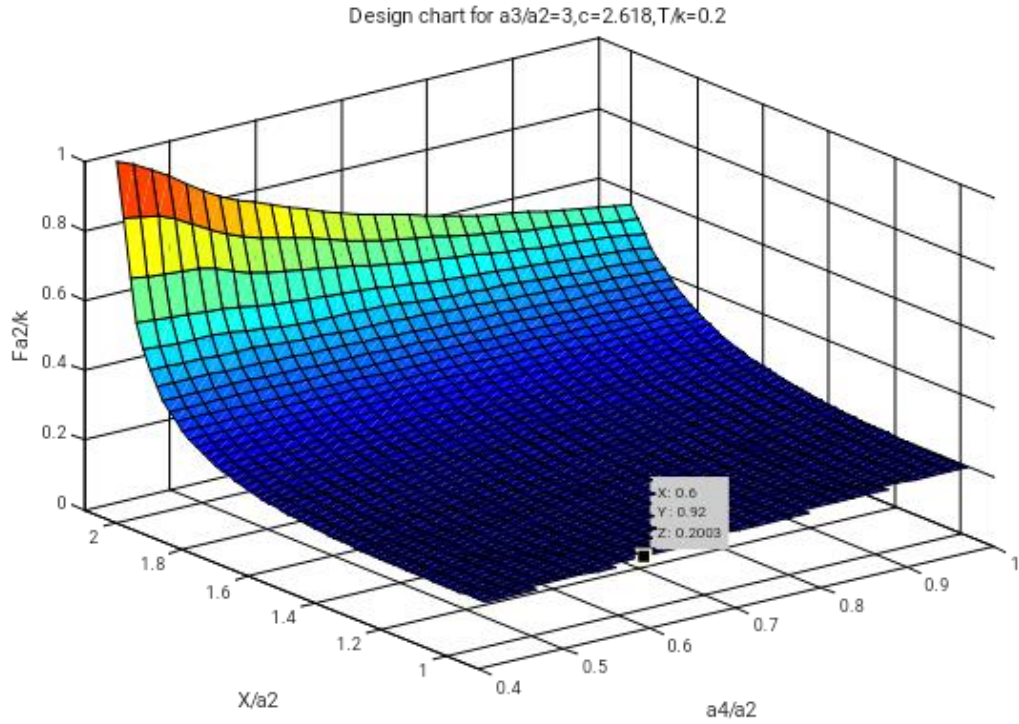


Figure 16 Data selection

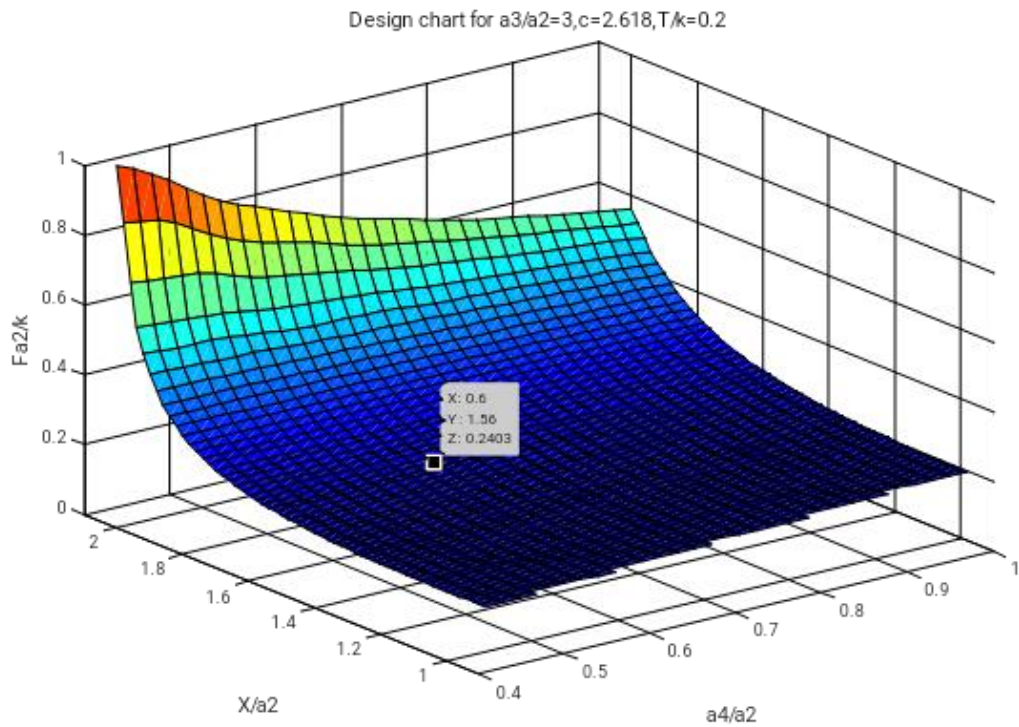


Figure 17 Data selection

Figure 18 and Figure 19;

$$\frac{a_4}{a_2} = 0.8 \rightarrow \frac{X}{a_2} = 0.94 \text{ to } \frac{X}{a_2} = 1.56$$

$$\frac{F * a_2}{k} = \sim 0.2 \text{ to } \frac{F * a_2}{k} = \sim 0.24$$

Hence $\frac{\Delta X}{a_2} = 0.62$

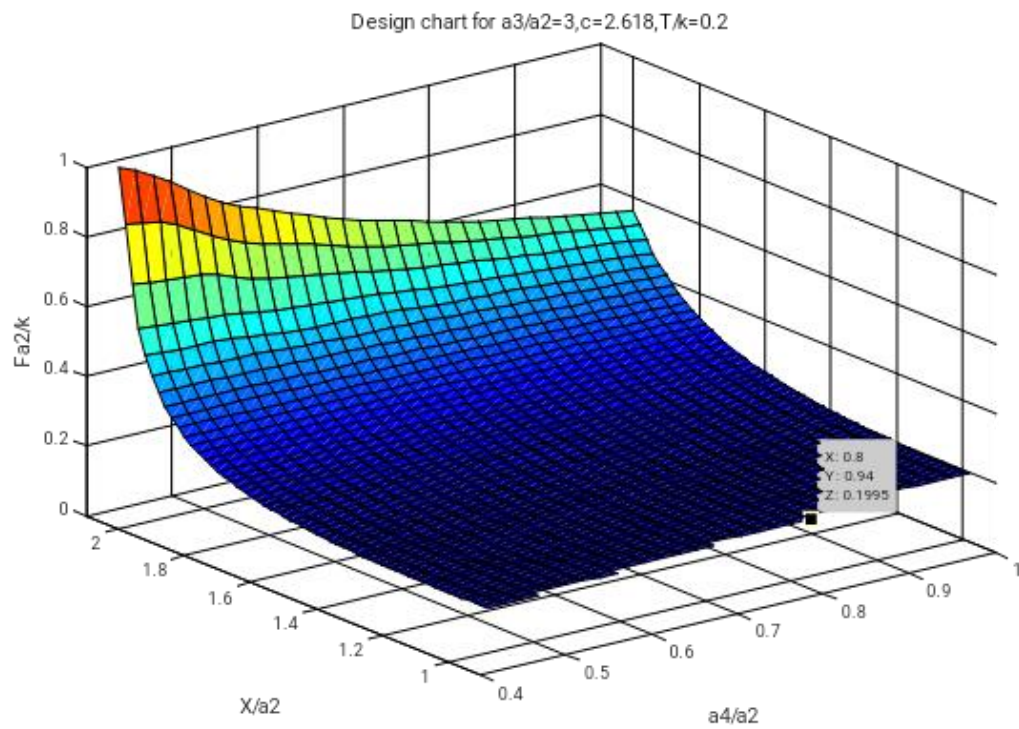


Figure 18 Data selection

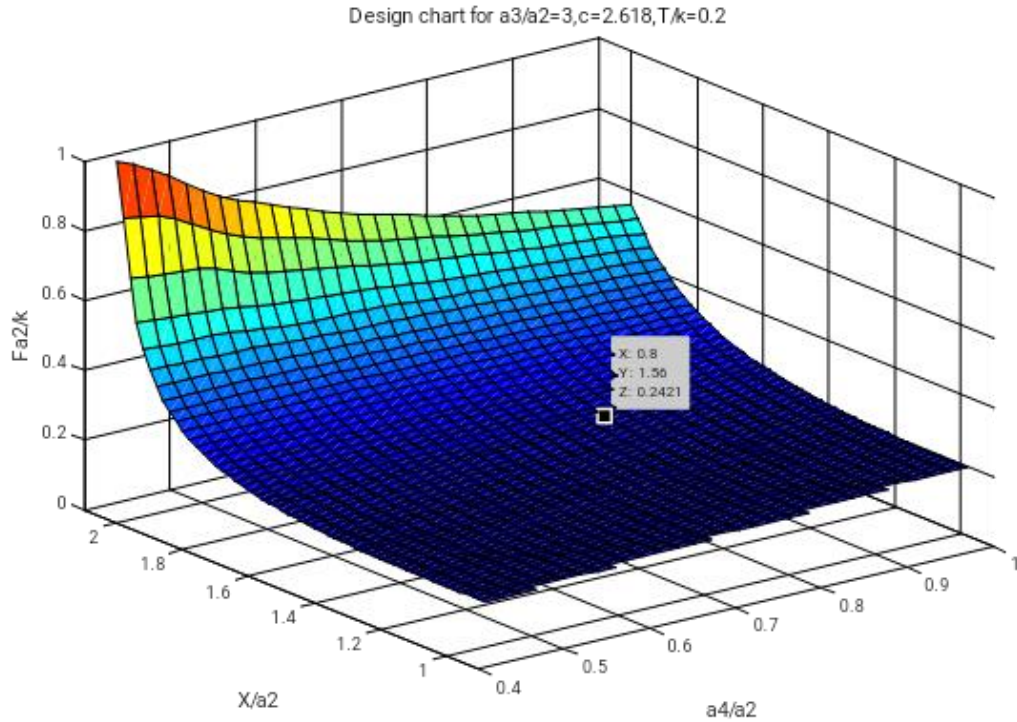


Figure 19 Data selection

The spring effect is calculated as given below,

Load factor is differentiated between 0 to 200 N as mentioned before, assuming the change in distance S_{15} in the elastic members assumed to be limited to %80 and the rotation applied to the spring bodies is up to 40° , the spring constants are estimated as follows,

$$2 * \left(\frac{1}{2} * k * \theta_{14}^2 \right) = F_{ave} * (0.1 * S_{15})$$

$$k * \left(40 * \frac{\pi}{180} \right)^2 = \left(\frac{100 + 90}{2} \right) * (0.1 * 410)$$

$$k = 2434 \frac{Nmm}{rad} = 2.4 \frac{Nm}{rad} = 2.4 \text{ kNmm/rad}$$

Hence the first assumption has been chosen for the initial step. Let the crank length $a_2=100$ mm. Then from the defined design charts $a_3=300$ mm and $a_4= 60$ mm. In this design option, the a_4/a_2 parameter has been selected as 0.6.

For the optimization mechanism behavior is analyzed with MATLAB function results Figure 14 [4]. Formerly, behavior of the mechanism analyzed with the given force

characteristics and there are some nearly constant region has been obtained. Second phase of this study is given constant torque behavior. Referring to Figure 14, first S_{max} and S_{min} values has to be determined and design chart is collected and tabulated. Code of this process is given in Appendix A – Matlab Code.

PRBM of the compliant gripper mechanism presented in Figure 20 the variable

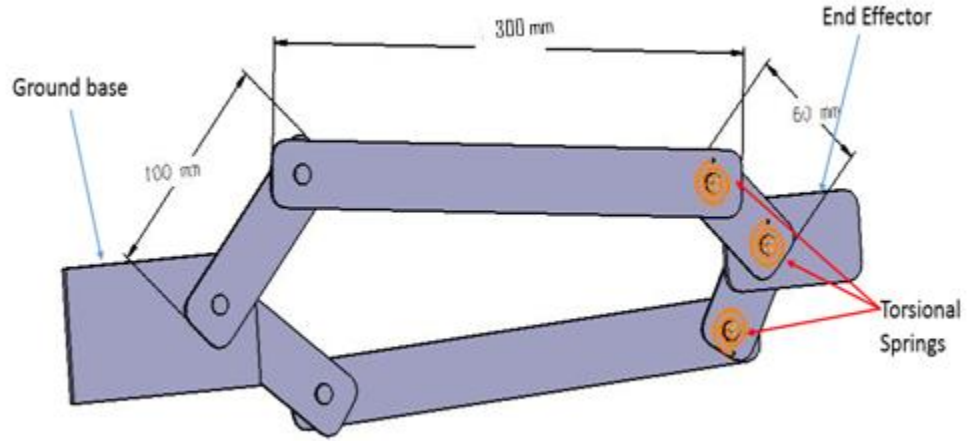


Figure 20 Pseudo Rigid Body Model

The proposed overall mechanism is presented in Figure 21. This mechanism is the rigid body equivalent of the compliant one. In the application various sized object could be handled by the compliant body replacement of this mechanism. In the initial position of the mechanism these torsional springs are at the unloaded position thus they are unstressed. In other words these springs are unloaded when applied torque on the related links are equal to zero. Hence the equations (11) and (12) have become as follows,

$$T_{34} = k_{34} * (\theta_{13} - \theta_{14} + c_{34}) \quad (11)$$

$$T_{45} = k_{45} * (-\theta_{14} + c_{45}) \quad (12)$$

$$T_{34} = k_{34} * (\theta_{13} - \theta_{14} + c_{34}) = 0 \quad T_{45} = k_{45} * (-\theta_{14} + c_{45}) = 0$$

From Figure 11 in the unloaded condition where $\theta_{12} = 0^\circ, \theta_{13} = 10^\circ$ and $\theta_{14} = 130^\circ$ observation may be carried out, and after substitution of the values into the equations,

$$(10 - 130 + c_{34}) = 0^\circ \rightarrow c_{34} = 120^\circ \text{ and } (-130 + c_{45}) = 0 \rightarrow c_{45} = 130^\circ \text{ (degree)}$$

To round up these parameters let $c_{45} = c_{34} = 125^\circ$ (degree)

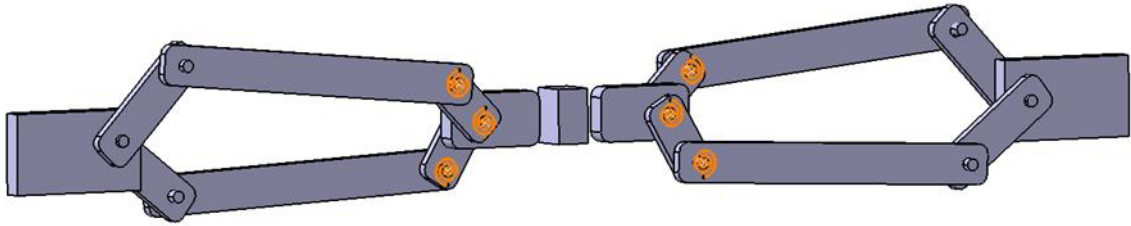


Figure 21 Rigid body counterpart of gripper mechanism

This mechanism presented in Figure 21 is the whole gripper mechanism. In the design procedure a mirror technique is applied thus the overall mechanism is reduced to a quarter section which is the same as the first section of the synthesis section, namely a variable stroke mechanism. In the real application of the mechanism, vertical forces of the gripper end effectors coming from the links are cancelled and the only applicable force is the horizontal one which is useful for grasping the objects, that's why the design is derived from the quarter section.

Within the selected parameters the rigid body replacement of the mechanism is as shown in Figure 22. In the figure, there is a compliant variable stroke under actuated mechanism, overlaid with the rigid body equivalent of the mechanism in the same place. In the compliant segments there are some curvatures which over-stressed due to the elasticity and the flexibility of the member.

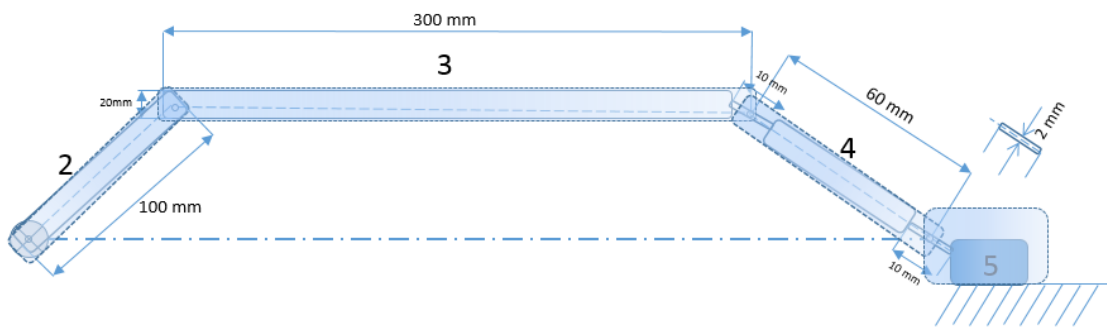


Figure 22 Rigid Body Replacement

2.2 Mechanical Properties

2.2.1 Material Selection

Material selection is another important feature of the design. Initially there are many materials that could be used in the design. However, a design of compliant mechanism based on elastic materials could be divided into two categories of nonlinearities. These are material *nonlinearities* and geometric *nonlinearities*. In this section I will mainly focus on the first characteristic, geometric characteristics detailed in the synthesis section of this study. Material *nonlinearities* based on Hooke's Law, which states that stress is proportional to strain is not applicable in such cases as plasticity, nonlinear elasticity, hyper elasticity, and creep. In literature, glass is known as very brittle and not flexible but a glass beam fabricated in small diameter and of enough length could behave in a flexible manner and not conform to conventional theory. Hence it could be stated that brittleness and flexibility are not necessarily related. Usually a brittle material will shatter when failure or yield stress is reached. However, ductile materials may continue to yield when stress goes beyond the yield strength. In material characteristics there are important factors known as stiffness and strength. Some ductile materials such as polypropylene may be stressed beyond their yield strength thousands of times without fracturing. In order to select the most appropriate materials for a compliant mechanism, devices and structures are chosen to maximize flexibility rather than stiffness.

There are some properties behavior divergence in metals and plastics. Metals have well-known material properties that perform in harsh and high temperatures environments, predictable fatigue life etc. Plastics have benefits such as electrical insulating, reduced assembly of parts, low density, low manufacturing costs, etc. However, plastics have some disadvantages such as low melting temperatures, creep and stress relaxations variance in material properties in sections or nonlinearities in elastic material properties. In order to strengthen the plastic based materials glass is frequently used for reinforcement. Table 3 provides a comparison of the mechanical properties of the selected metals and plastics.

Table 3 Ratio of yield strength to Young's modulus for several materials

Material	E [Mpsi]	E [Gpa]	S _y [kpsi]	S _y [Mpa]	(S _y /E)*1000
Steel (1010 hot rolled)	30	207	26	179	0.87
Steel (4140 Q&T@400)	30	207	238	1641	7.9
Aluminum (1100 annealed)	10.4	71.7	5	34	0.48
Aluminum (7075 heat treated)	10.4	71.7	73	503	7.0
Titanium (Ti-35A annealed)	16.5	114	30	207	1.8
Titanium (Ti-13 heat treated)	16.5	114	170	1170	10
Berlyllium copper (CA170)	18.5	128	170	1170	9.2
Polycrystalline silicon	24.5	169	135	930	5.5
Polyethylene (HDPE)	0.2	1.4	4	28	20
Nylon (type 66)	0.4	2.8	8	55	20
Polypropylene	0.2	1.4	5	34	25
Kevlar (82 vol %) in epoxy	12	86	220	1517	18
E-glass (73.3 vol %) in epoxy	8.1	56	238	1640	29

Polypropylene is the most appropriate polymer to use in the design because; it has advanced ratio of strength to modulus as given in Table 3, it is easily acquirable, inexpensive, easy to process and has a low density. Additionally, it is very ductile and when yielded results in less catastrophic failure. In conclusion, it is an outstanding and commonly used material in compliant mechanisms.

2.2.2 Stress and Force

In the problem statement, the initial estimate of the link length are $a_2=100$ mm, $a_3=300$ mm and $a_4= 60$ mm and the design chart reference the $\frac{T}{k} = 0.2$ and $k = 5.8$ kNmm/rad hence the applied torque is 0.5 Nm.

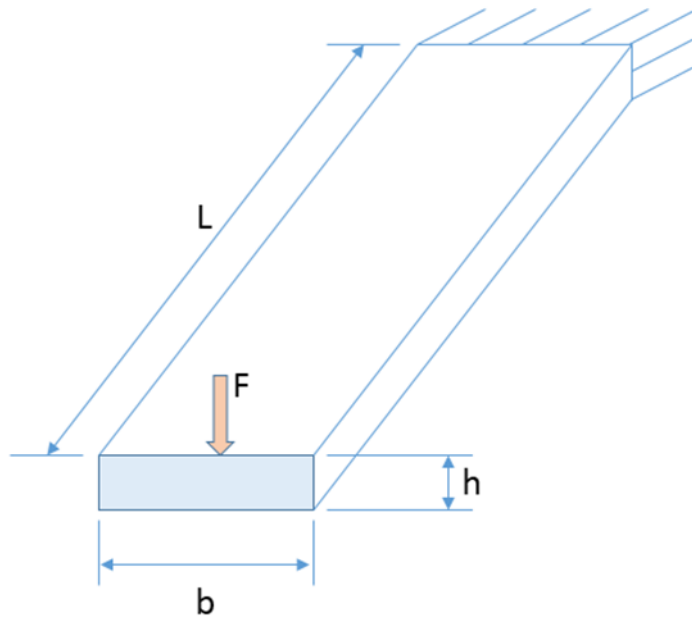


Figure 23 Generic Rectangular Beam Cross Section

The next step is to decide the width (b) and the thickness (h) values given in the generic sketch on Figure 23. Let width $b = 20 \text{ mm}$ and thickness $h = 10 \text{ mm}$ in the links. In the coupler part of the link is 60 mm and both ends are connected with the torsional springs in the PRBM. To convert and adapt them to the compliant mechanism flexible segments are used for the flexural pivots let the flexural parts length are 10 mm each then the coupler part length is totally 70 mm.

The flexural pivot part 10 mm length and the presumed width is 2mm and the depth is the same as the other links (i.e. equal to 10mm). In the analysis section due to the more appropriate results and easy to manufacturing grooving with a circle of the body these super-precision link connectors as a flexural pivots could be differentiate.

Then in the flexural pivots

$$k = \frac{EI}{l} ; I = \frac{1}{12}wb^3$$

Substituting the values by selecting typical polypropylene where $E = 1400 \text{ Mpa}$. Using the values for the flexural pivots

$$I = \frac{1}{12} * 10\text{mm} * 2\text{mm}^3 = \frac{80}{12}\text{mm}^4$$

$$k = \frac{EI}{l} \rightarrow l = \frac{EI}{k} = \frac{1400\text{Mpa} * \frac{80}{12}\text{mm}^4}{\frac{5800}{2 * \pi}\text{Nmm}} \cong 10\text{mm}$$

The length of the flexural pivots is 10 mm and the coupler link total length is 70mm. The compliant mechanism can be synthesized based on the PRBM as presented in Figure 24.

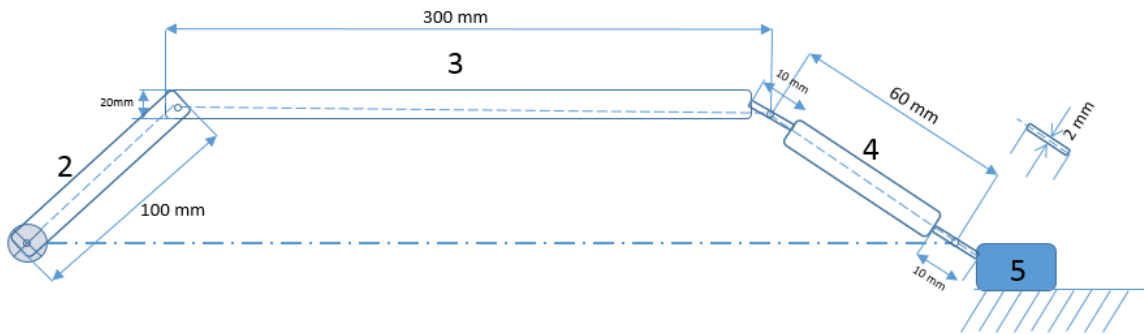


Figure 24 Compliant mechanism based on the PRBM

2.3 Optimization

In order to design a compliant mechanism, the flowchart in Figure 25 is given to explain the procedure, some steps of this procedure have already been completed. The specification is determined to create a mechanism to grip various sized objects with constant force. Rigid body model synthesis has been completed with related calculations of the parameters. Additionally, PRBM has been constructed with replacement torsional springs on the mechanism, the mechanism is refined using the quarterly design and stress, strain, and life feasibility are calculated with as shown in the flowchart The design process flow charts are adapted from [5].

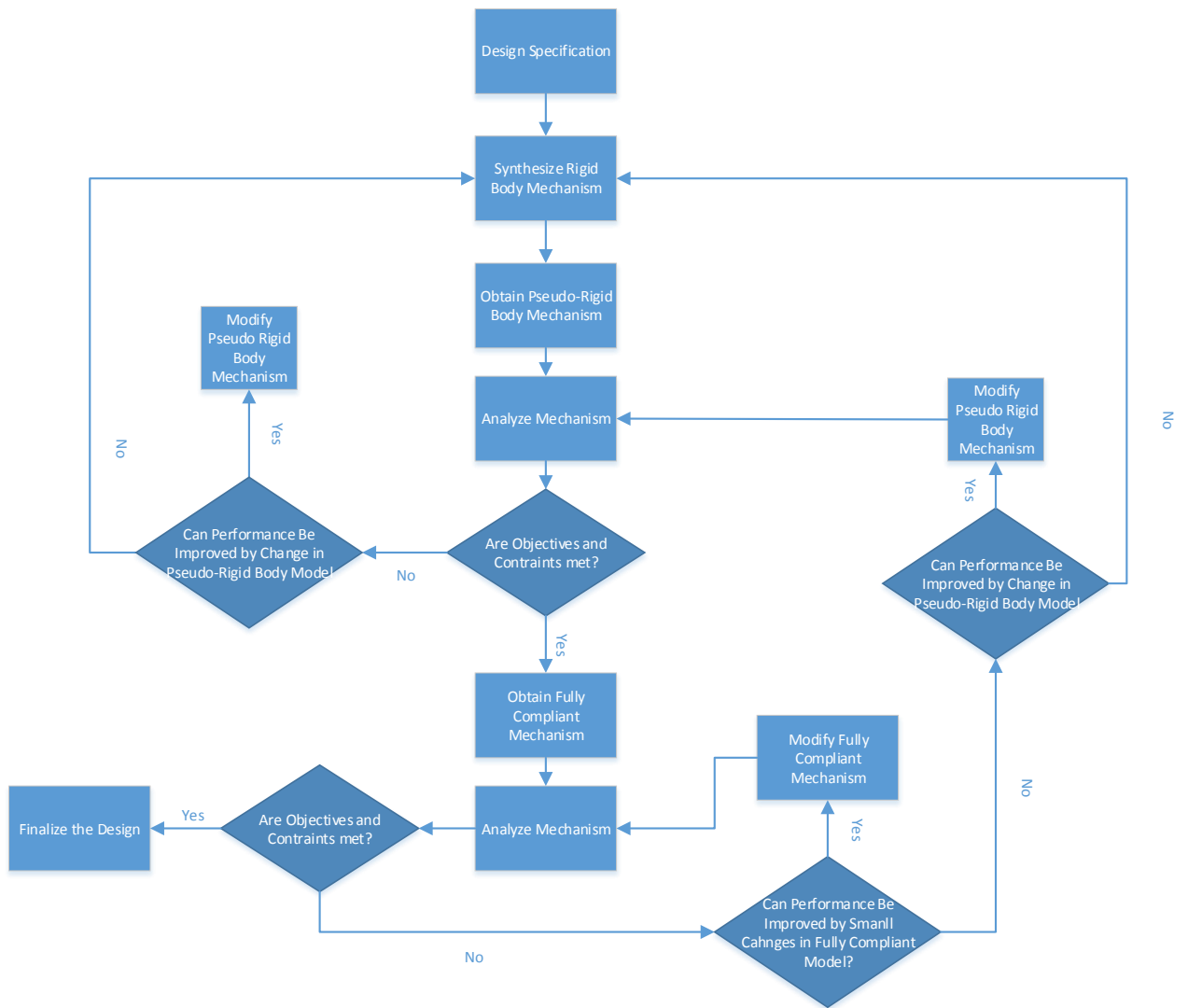


Figure 25 Compliant Mechanism Design Process [5]

3 ANALYSIS AND VERIFICATION

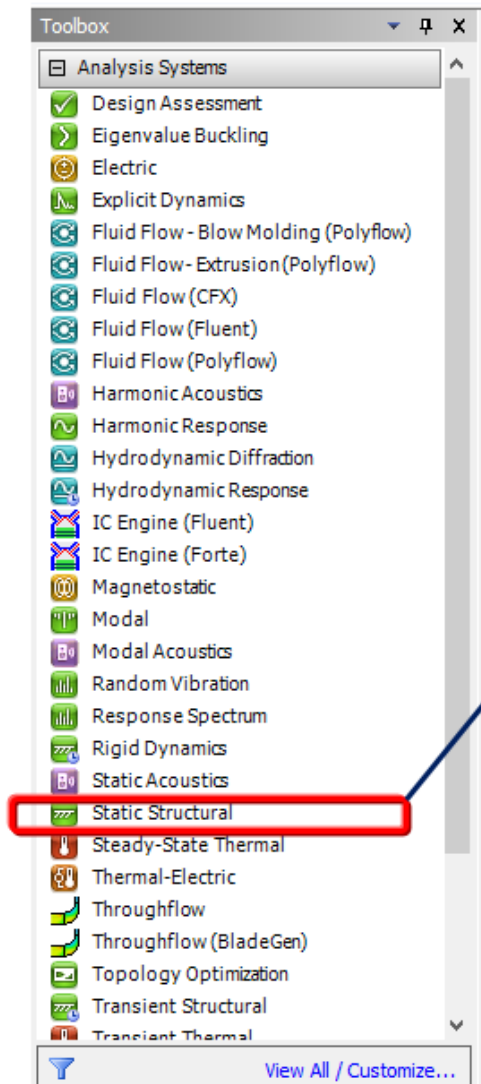
3.1 Introduction of analysis

In the analysis section of this study, the ANSYS is used. The torque input of the system, which has been defined earlier in the design chart, is calculated using the following calculation:

$$\frac{T}{k} = 0.2$$
$$k = 2.4 \frac{kNmm}{rad} \rightarrow T \cong 0.5 \frac{kNmm}{rad}$$

The geometry is drawn as a CAD file and exported as STEP file format. Analysis is done using ANSYS, the Static Structural module is used as shown below Figure 26. Static Structural module is preferred due to the mathematical calculation is derived concerning with static equilibrium in time. Finite element method is used by this module. Apart from that transient structural module could be used for dynamic analysis within the related mathematical formulations and calculations in this case, force calculation is depends on the acceleration parameters of the system behavior.

Following steps are using for proceeding of the ANSYS as given below;

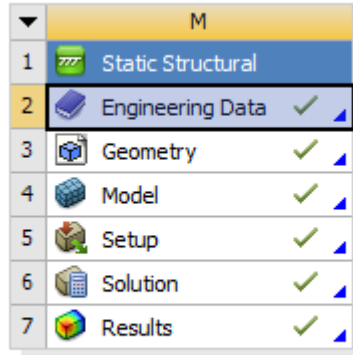


Analyzing systems box is opened when ANSYS is started for determining the analyzing module (Static Structural, Dynamic or Transient Analysis, Thermal Analysis etc.).

In this paper Static Structural Module is used in order to obtain the proper results aligned with the previous mathematical calculations.

Figure 26 ANSYS Workbench opening window

After opening the Static Structural module, in Engineering Data section material properties are defined. In this section program has tremendous library about different kind of material properties.



Quarter Model Static Structural with chart

Figure 27 Opening Engineering Data Assignment

In case specific material density, temperature, Young's Modulus, Poisson's Ratio, Bulk Modulus, Shear Modulus, Tensile and Compressive Yield Strength and Tensile or Compressive Ultimate Strength parameters can be defined with project or material specific. Clicking on the Engineering Data section as given Figure 27 known parameters assigned in combo-boxes with units assignment depicted in Figure 28.

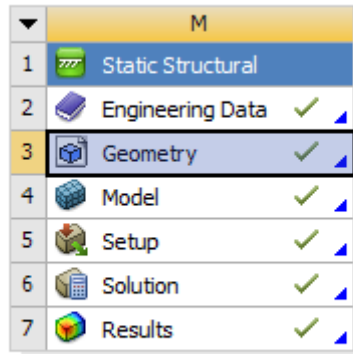
	A	B	C	D	E
1	Variable Name	Unit	Default Data	Lower Limit	Upper Limit
2	Temperature	C	22	Program Controlled	Program Controlled

	A	B	C	D	E
1	Property	Value	Unit		
2	Material Field Variables	Table			
3	Density	7850	kg m ⁻³		
4	Isotropic Elasticity				
5	Derive from	Young...			
6	Young's Modulus	1400	MPa		
7	Poisson's Ratio	0,36			
8	Bulk Modulus	1,6667E+09	Pa		
9	Shear Modulus	5,1471E+08	Pa		
10	Tensile Yield Strength	32,8	MPa		
11	Compressive Yield Strength	10	MPa		
12	Tensile Ultimate Strength	79,7	MPa		

Figure 28 Engineering Data Assignment

3.2 Geometry

Next step is geometry creation and as previously mentioned geometry is drawn with Solid Works 2018 and exported with STEP file. In ANSYS software program, geometry is imported with this STEP file with right click on the geometry section specified in Figure 29.



Quarter Model Static Structural with chart

Figure 29 Geometry Section

Within concerning the geometry specified before the quarter analysis geometry is defined as given Figure 30. Proposed geometry defined in early sections (synthesis) of this study is used for analysis section.

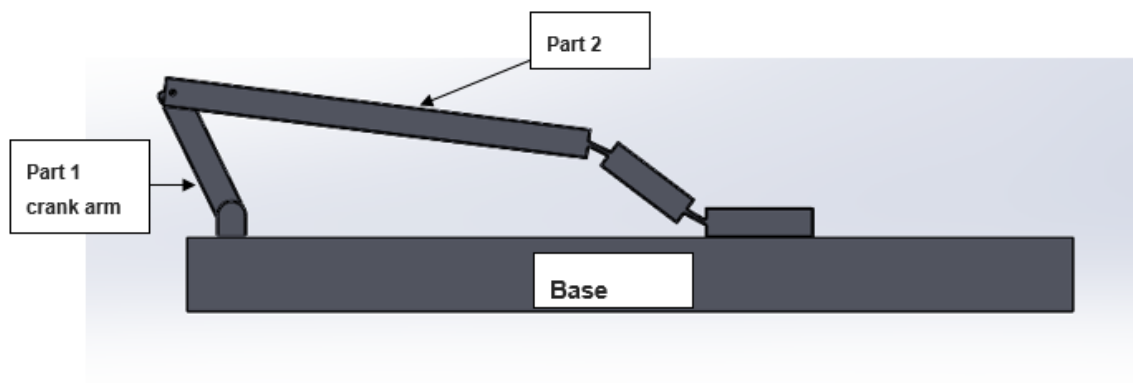


Figure 30 Quarter-Geometry front view in Solid Works 2018

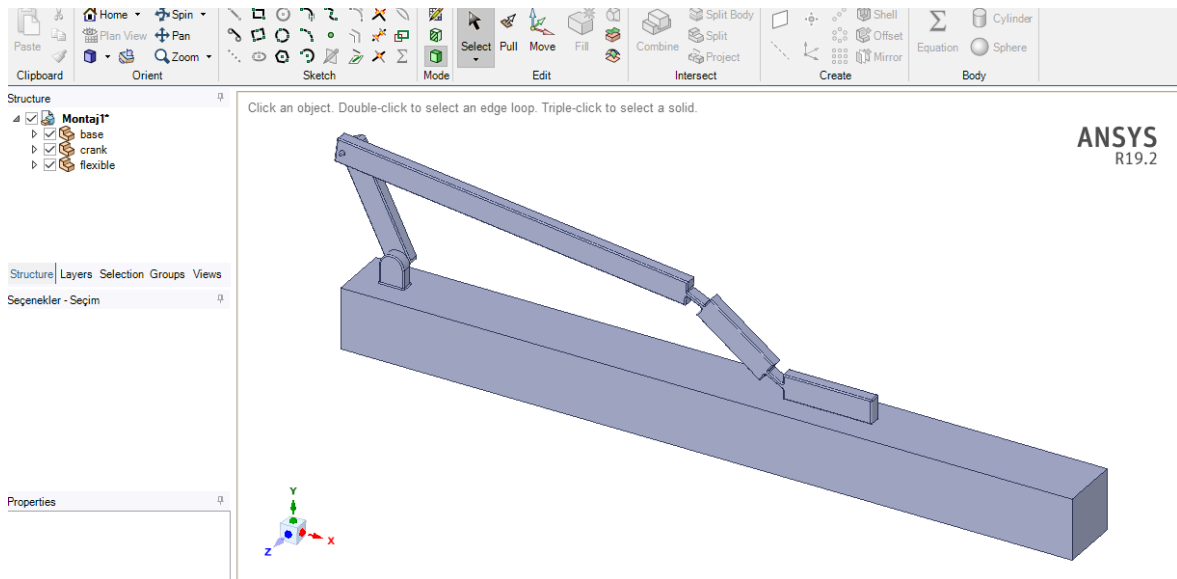


Figure 31 ANSYS Geometry Generation

The geometry consists of two rigid links, one compliant link and two revolute joints. There are two initially straight compliant segments available in the compliant link. The dimensions are given at Figure 22. The thickness of the two compliant segments is 10 mm. Link 1 which is crank arm, is attached to link 2 and the base with revolute joint.

In this analysis, half of the mechanism is also decided to analyze to compare the results are aligned with or not. The half mechanism geometry is depicted in the Figure 32. It is created as mirrored of the quarter body model.

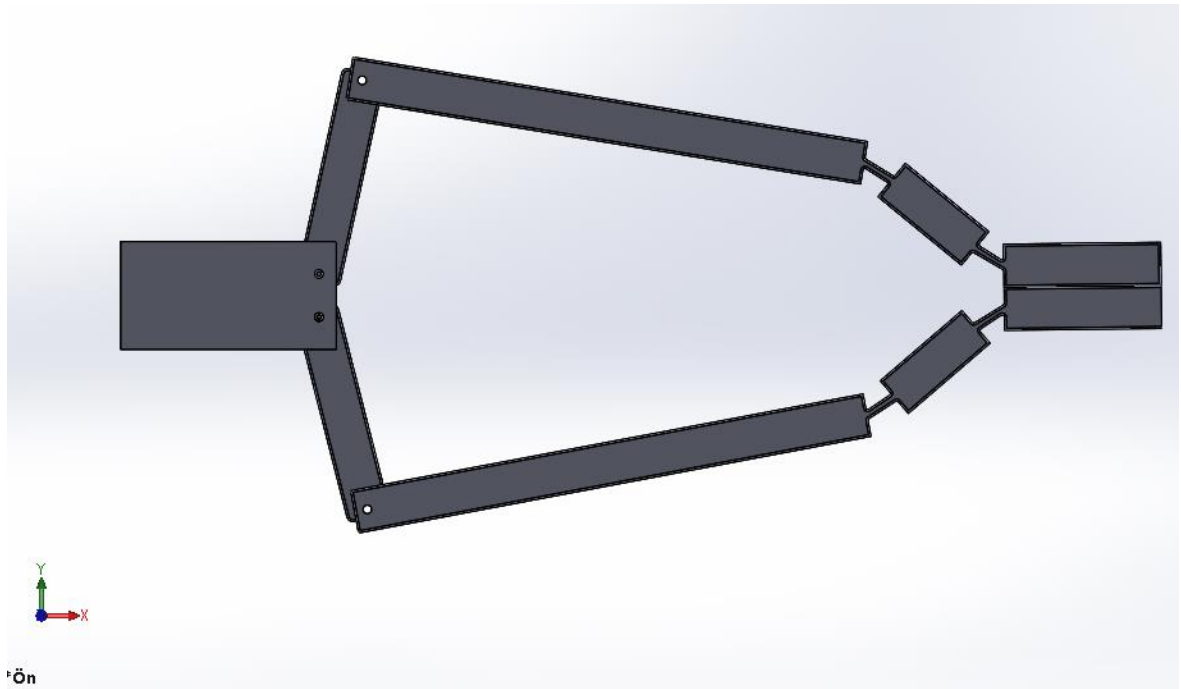
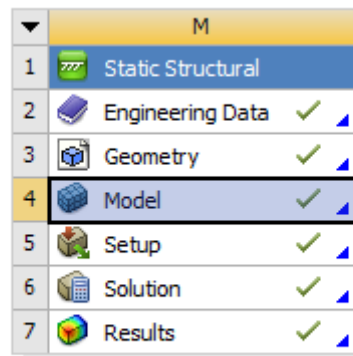


Figure 32 Half-body geometry front view in SolidWorks2018

3.3 Model and Analysis Section

After completion of the geometry section, ANSYS Model section opens and analysis settings are identified depicted in Figure 33.



Quarter Model Static Structural with chart

Figure 33 Model Section

Materials are assigned to each part of the geometry as defined earlier structural steel or polypropylene shown in Figure 34. Base of the geometry is suppressed to work and analyse the mechanism in less time or less power consumption.

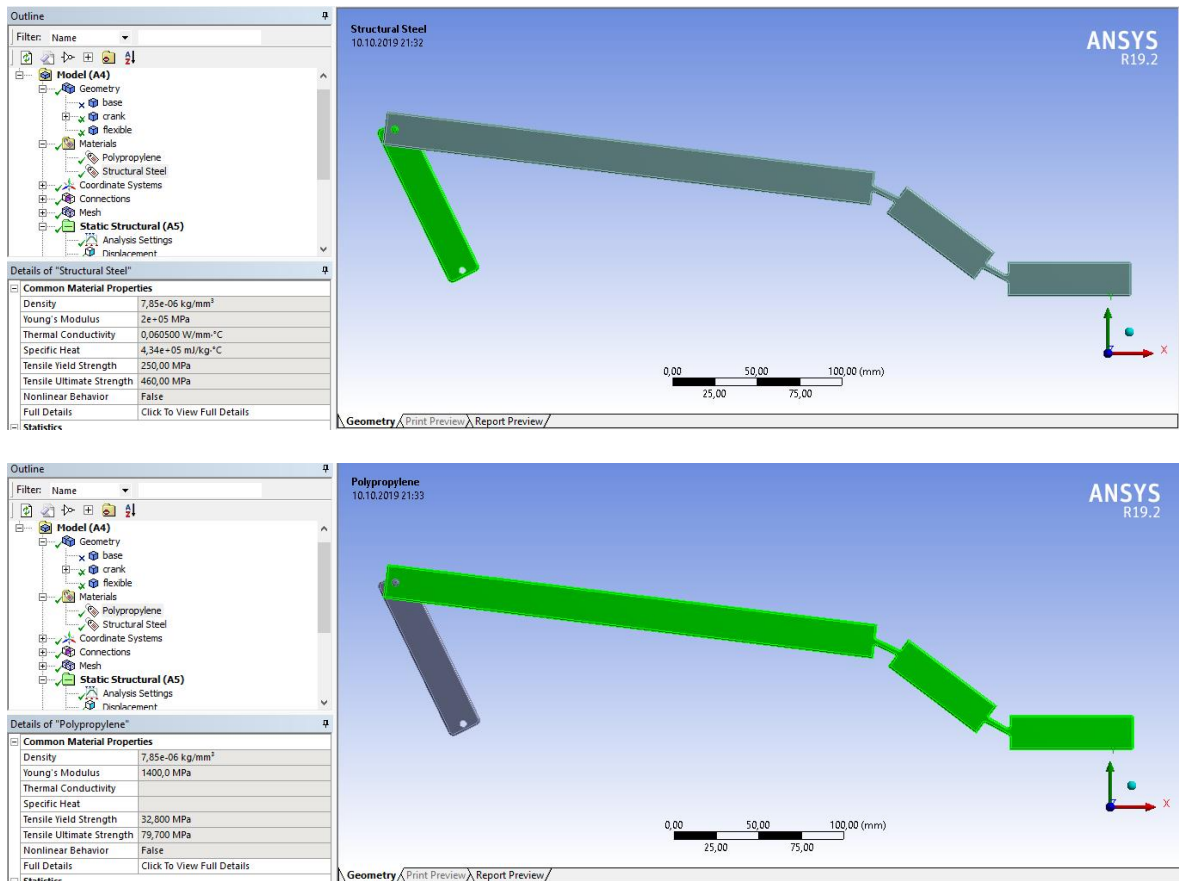


Figure 34 Material Assignments on Parts

In ideal case and mathematical calculation, there is no contact force assumed hence contact section is suppressed. In connection section, only the revolute joints and translational slider joints are specified depicted in Figure 35 .

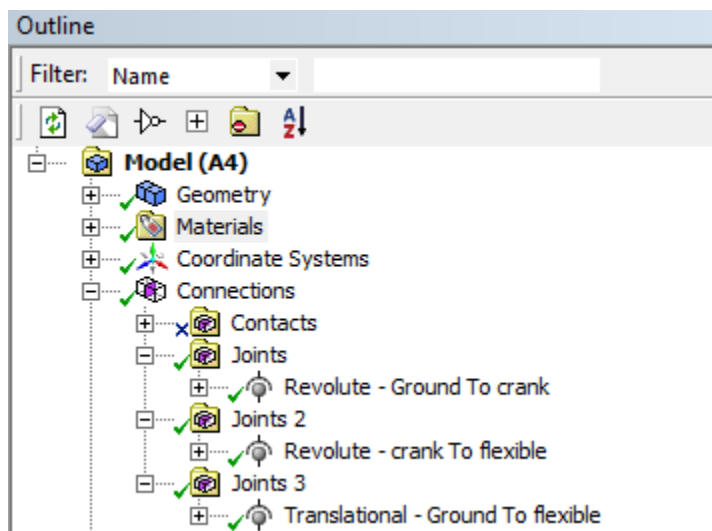


Figure 35 Joint Type Assignment

In the quarter geometry, analysis an automatic mesh is used with 'Body Sizing' option giving order of 0,005. The mesh independency case is studied and convergence of the results is obtained. The mesh independency studies show that after 22000 nodes the result does not change. The node number is specified as 17000). The meshed quarter mechanism is given in the Figure 36.

Mesh independency and mesh sensitivity is the one of the popular subjects for the ANSYS analysis work package. It is widely used for CFD applications for specific purposes of turbine blade design specification and the load distribution of fluid in contact with the mechanism interfaces. In this study specific applications interfacing with fluid are of no matter, but the mesh node correction is more appropriate, the mesh independence and sensitivity are important in this particular design. Probe is used to determine the force on the slider.

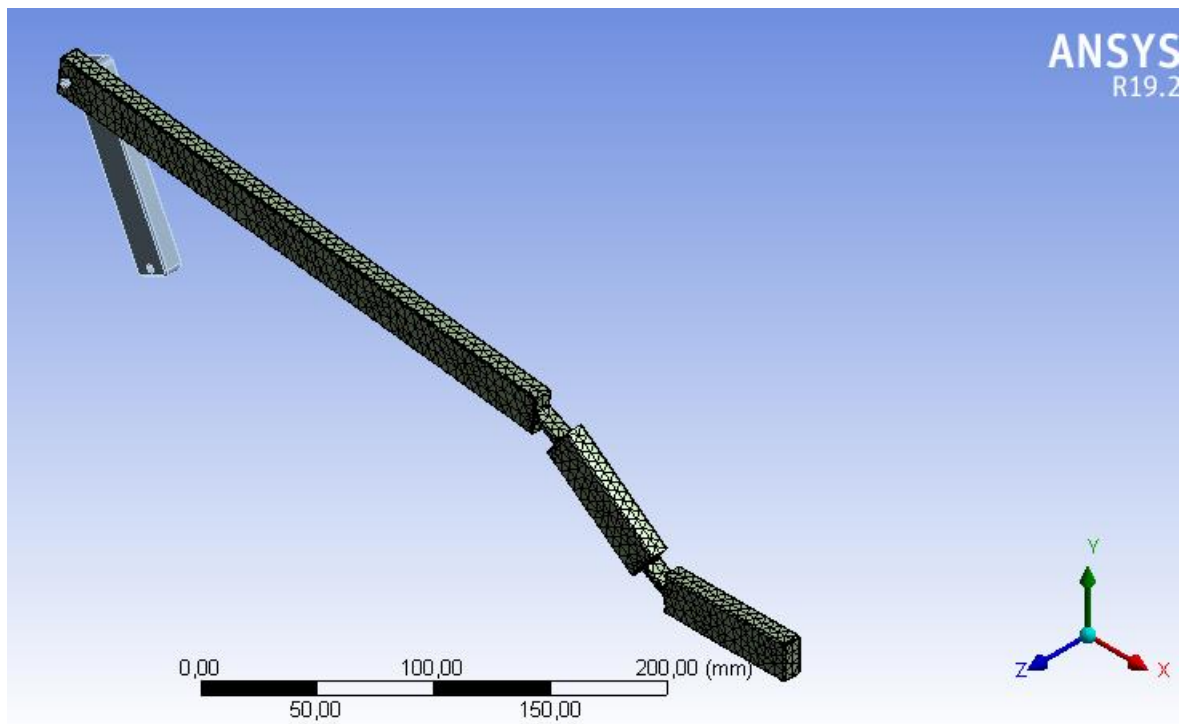


Figure 36 Mesh analysis of the quarter mechanism

The half range application meshed mechanism is shown at Figure 37.

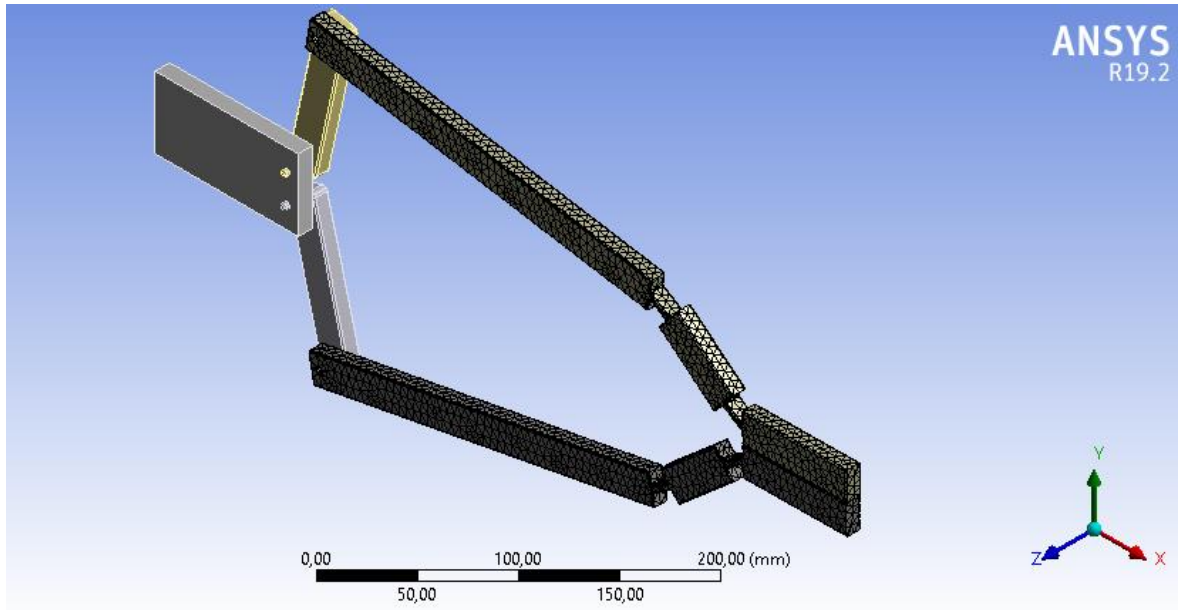


Figure 37 Mesh analysis of half mechanism

In the mesh independence analysis of the system, the mesh node number is enough to analyze the system. It is not required that the mesh node number increase.

3.4 Analysis Preprocessing

Analysis is prepared a static structural module and geometry is imported. In ANSYS transient structural analysis enables to analyze rigid or flexible systems with dynamic responses on the mechanism includes stresses under the time depending loads or time varying displacements. Stresses, strains, forces, and displacements in the mechanism includes in static structural analysis. Another advantage of static structural analysis is that it enables to linear or non-linear deformation or behavior of the system hence it is useful to apply on the compliant system analysis. Joints are created as concerning the parameters defined in the Table 4:

Table 4 Part number and joint type compliance for Quarter-Geometry

Joint number	Part numbers	Type of joints
1	ground and crank	Revolute
2	crank and flexible part	Revolute
3	slider and ground	Translational

All joint types and freedom characteristics are defined in the section 1.3.1 in this thesis.

At joint number 1 is charged with leading to moment as 0.5 Nm for direction CCW and initial position is specified in Figure 38. In Analysis settings variable are defined as follows,

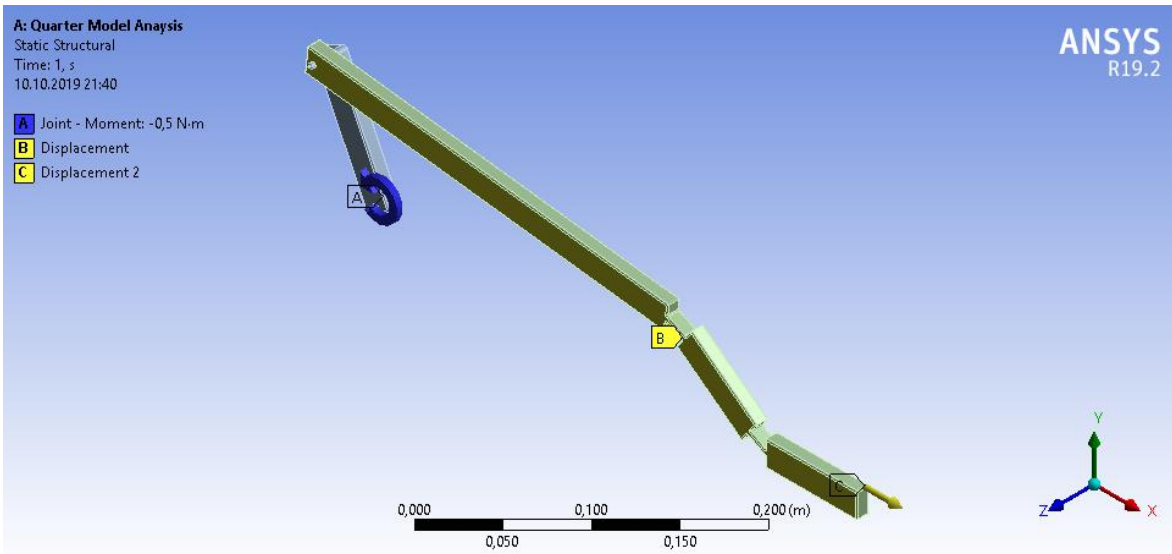


Figure 38 Analysis Inputs

Apart from the 0,5 Nm torque input of the system there are some other boundary conditions have to be specified. The first one is given on the Figure 38 as B is the displacement of the polypropylene part deflection in Z direction is restricted to avoid the buckling effect and given in the software with tabular form as 0 (zero) in Z direction. The second one is given as C is the displacement characteristics of the slider and it is given

as tabular form in ten steps increasing with the same values derived from theoretical results it could be said that the mean value of 5,5 mm. At the end of the analysis the results are compared with the MATLAB results.

Details of "Analysis Settings"	
Step Controls	
Number Of Steps	10,
Current Step Number	1,
Step End Time	1, s
Auto Time Stepping	On
Define By	Time
Initial Time Step	1,e-002 s
Minimum Time Step	1,e-003 s
Maximum Time Step	1, s
Solver Controls	
Solver Type	Program Controlled
Weak Springs	Off
Solver Pivot Checking	Program Controlled
Large Deflection	On
Inertia Relief	Off
Rotordynamics Controls	
Restart Controls	
Nonlinear Controls	
Output Controls	
Analysis Data Management	
Visibility	

Figure 39 Analysis Settings

In the solver control section under the analysis settings depicted in Figure 39, "Large Deflection" is selected as 'On' due to the nonlinear solving is required. Then the solution could be started, obtained output results displayed as Figure 40 after the solution run properly.

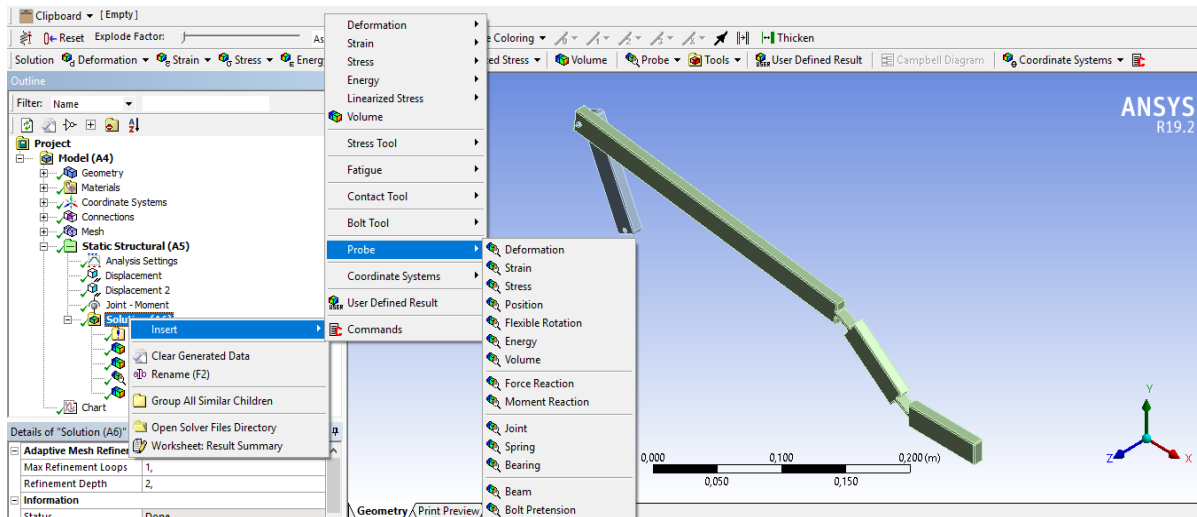


Figure 40 Output Results Selection

3.5 Results

The result of the force probe on the slider is created and the force which is acting on this part is obtained. Equivalent stress on the flexible part is obtained in the presumed region presented in Figure 41.

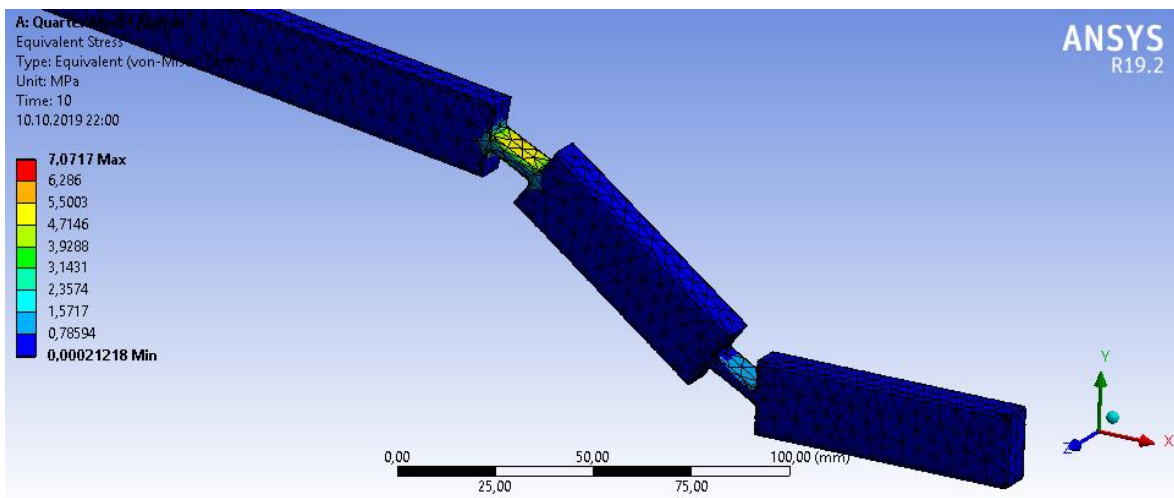


Figure 41 Equivalent Stress

The force output in the system and displacement characteristics is obtained with using a chart in ANSYS as given Figure 42,

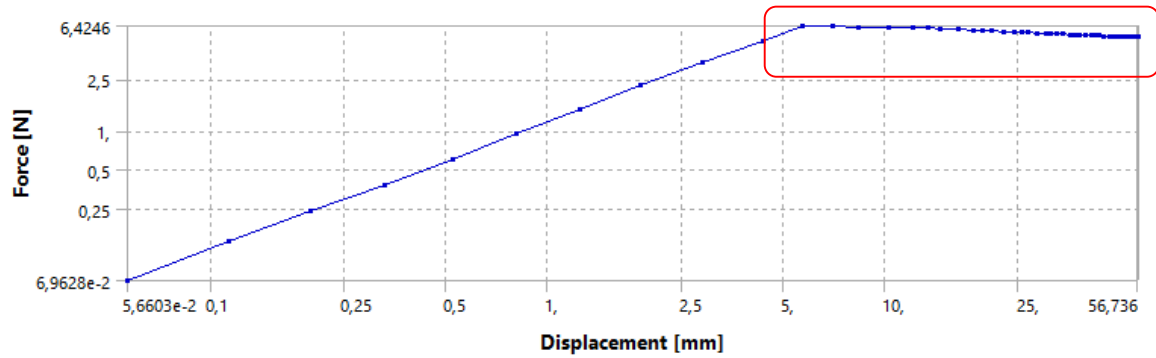


Figure 42 Force creation in X direction on the slider, ANSYS chart

The behavior of the mechanism is analyzed and the constant force range is derived in the angle range between distances. As observed from Figure 42 there is a nearly constant force region in the system in the range of the 5 to 55 mm displacement in 10 steps started on position of the slider is evaluated starting point in the calculation in ANSYS.

Additionally, the results both theoretical and simulation are evaluated with steps and concerning the starting point of the simulation calculation in ANSYS results are begin with crank angle of 117 degree and it is the 10th step, the results are defined in Table 5;

Table 5 Tabular Form of MATLAB and ANSYS Results

steps	MATLAB			ANSYS		
	Crank Angle (MATLAB) [deg]	Reaction Force (MATLAB) [N]	Displacement X (MATLAB) [mm]	Crank Angle (ANSYS) [deg]	Reaction Force (ANSYS) [N]	Displacement X (ANSYS) [mm]
	163,21	19,81	200,16			
	155,25	14,04	194,38			
	147,32	10,94	188,61			
	141,32	9,15	182,83			
	135,52	8,00	177,28			
	130,25	7,22	171,28			
	125,40	6,65	165,51			
	120,89	6,23	159,73			
1	116,63	5,90	153,96	116,94	6,2998	156,25

steps	MATLAB			ANSYS		
	Crank Angle (MATLAB) [deg]	Reaction Force (MATLAB) [N]	Displacement X (MATLAB) [mm]	Crank Angle (ANSYS) [deg]	Reaction Force (ANSYS) [N]	Displacement X (ANSYS) [mm]
2	112,59	5,76	148,18	111,91	6,2889	148,04
3	108,72	5,66	142,41	107,83	6,0819	141,42
4	105,00	5,32	136,64	103,79	5,834	134,93
5	101,40	5,20	130,86	100,03	5,6866	128,91
6	97,90	5,11	125,09	96,38	5,547875	123,12
7	94,48	5,05	119,31	92,72	5,452025	117,37
8	91,12	5,01	113,54	89,16	5,371775	111,81
9	87,82	4,99	107,76	85,62	5,308	106,36
10	84,56	4,99	101,99	82,08	5,281575	100,96
	81,33	4,99	96,00			
	78,11	5,02	90,44			

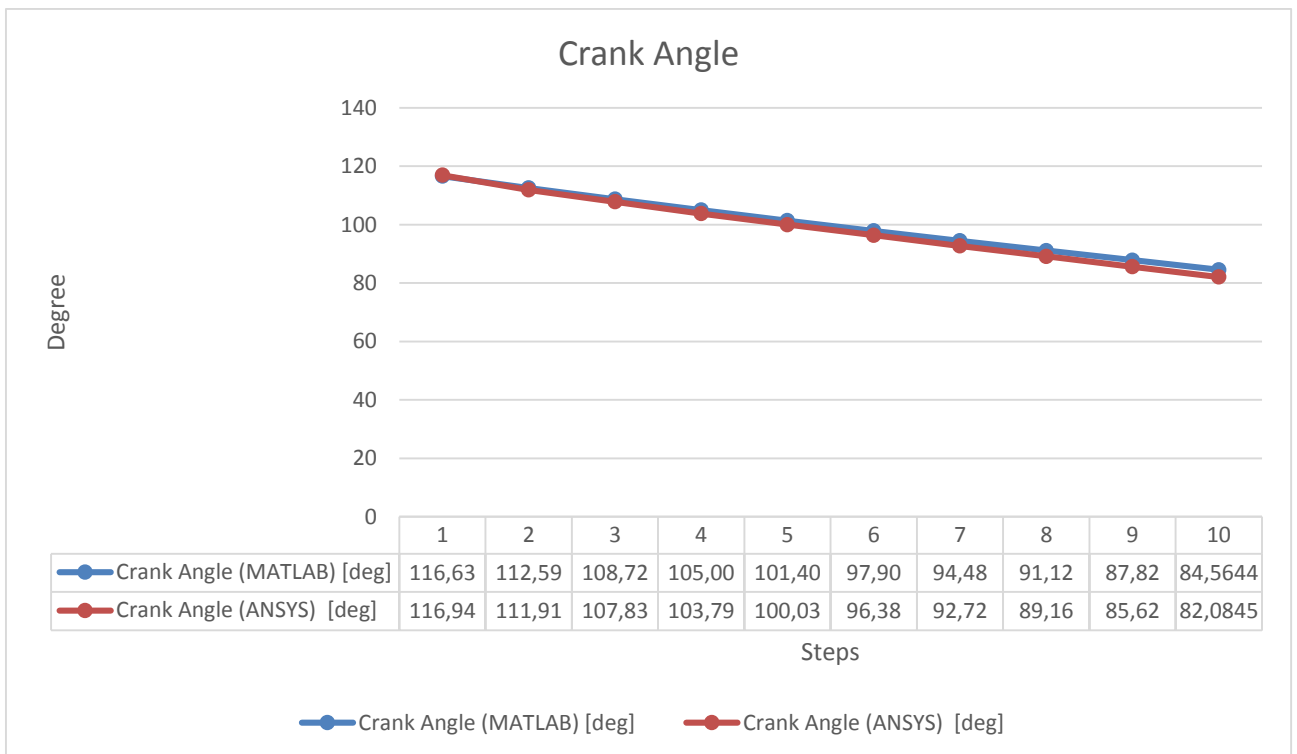


Figure 43 Results Comparison - Crank Angle

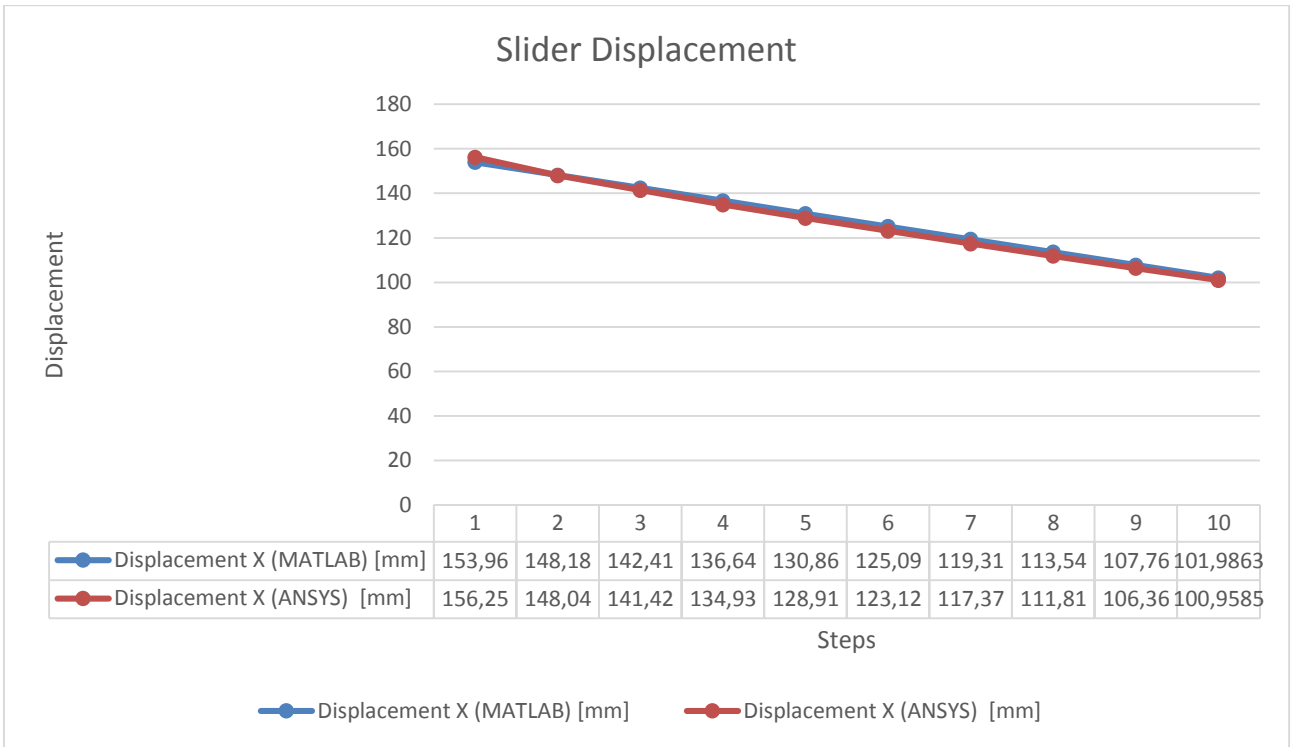


Figure 44 Results Comparison - Slider Displacement

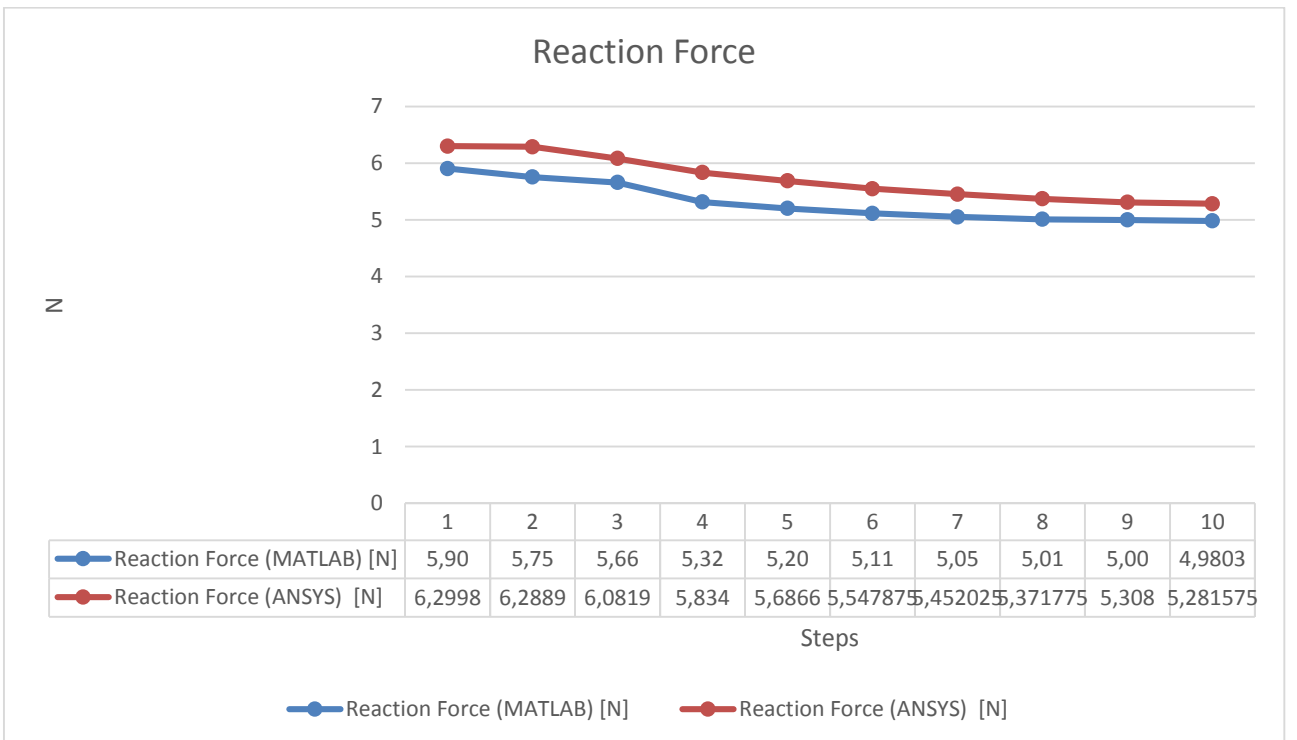


Figure 45 Results Comparison - Reaction Force

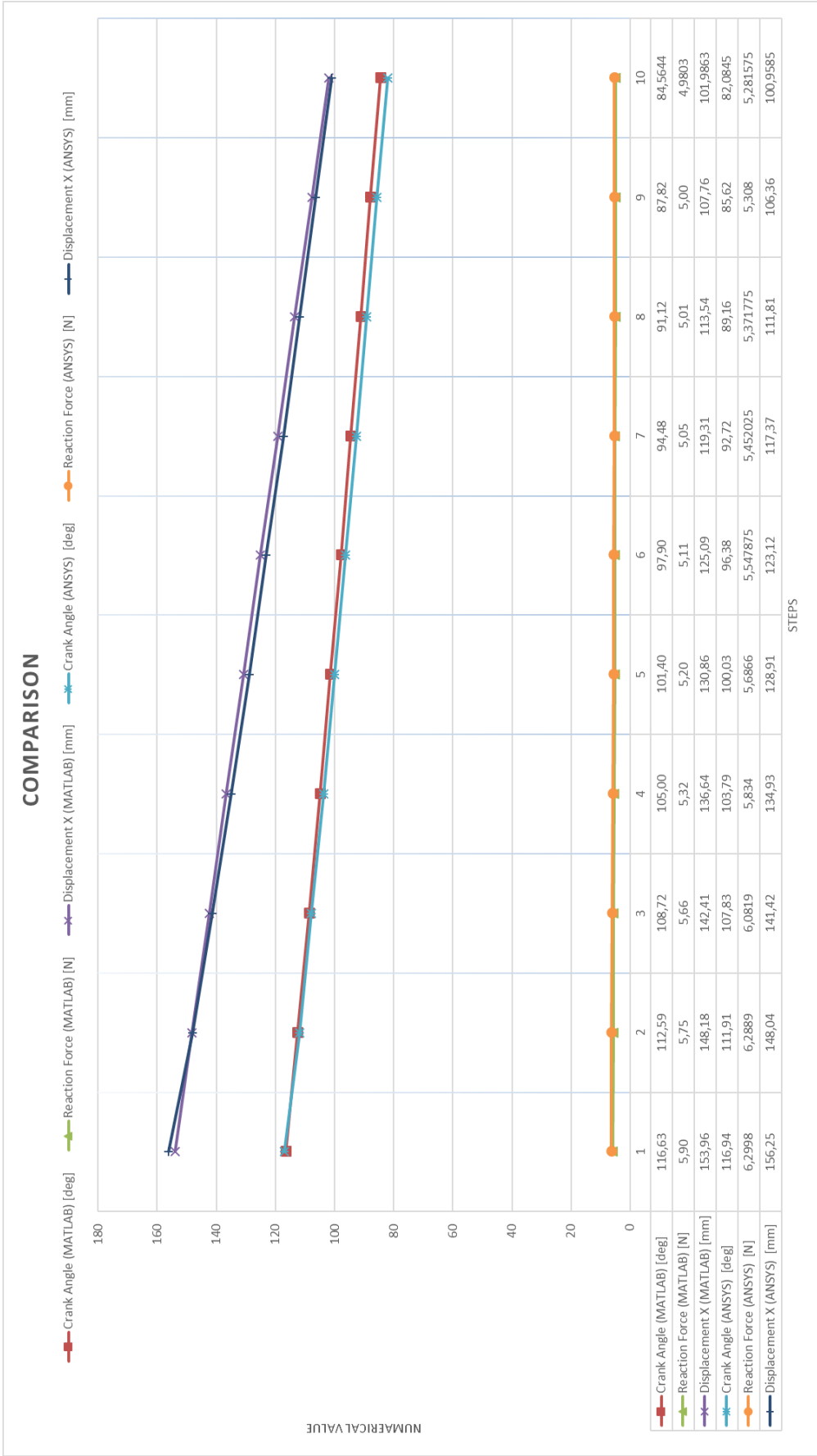


Figure 46 Results Comparison

In both mechanisms analyses, there are crank angle changes, slider displacement and output force as constant force ranges that have been observed with nearly 10 percent deviation as shown Figure 43, Figure 44, Figure 45 and Figure 46 Results Comparison.

4 CONCLUSION

Tremendous previous studies in literature on the constant force compliant mechanism has been absorbed prior to this thesis. To find out the proper mechanism basis for designing constant force compliant gripper mechanism, a compliant variable stroke mechanism has been designed. The theoretical results indicated that there are constant ranges within the changing crank angle in either output angle or the slider motion. It initiates to design a mechanism that can be constant output force range and based on this approach, non-dimensional parameters are studied in order to obtain design charts. Constant force characteristics are shown as a flat region on the design charts elementarily. Considerations focus on the validation and verification of the theoretical outputs. For this reason, gathering some points on the design chart and selecting one of them length, thickness and width values are defined for using as inputs for validation processes.

By using a proper software program for validation processes, results are obtained similar with initial theoretical approaches and assumptions. Due to the ten steps solution results availability in ANSYS, counterparts of the theoretical one that is evaluated via MATLAB are compared. Comparison shows that deviations do not exceed % 2 in crank angle results. Likely displacement values have been gathered from the simulation results are nearly similar to the theoretical ones. Variation of displacement do not exceed % 2 when compared. Force reaction results between the theoretical and simulated ones have some discrepancies at some points but not exceeding % 10 at values and therefore, it is acceptable for design cases.

To sum up, the presumed selected data values of the compliant mechanism have been analyzed using ANSYS software package and both solution and data results are consistent with the initial theoretical results that create constant force range. There is a slider motion range with a constant force output, the results of the analysis enable us to handle various sized objects with constant torque inputs on the crank of the mechanism generating constant force outputs.

5 REFERENCES

- [1] Anonym, pictures from <https://goo.gl/images/VeNU4r> , <https://goo.gl/images/ZmYRSc> , <https://goo.gl/images/F8kjuR> and <https://goo.gl/images/XWZBge> (Access date: **14 May 2018**)
- [2] Chang, L. H., and Fu, L. C., “Nonlinear adaptive control of a flexible manipulator for automated deburring,” *Proceedings - IEEE International Conference on Robotics and Automation*, Vol. 4, pp. 2844-2849, **1997**.
- [3] Chao-Chieh Lan and Jhe-Hong Wang, “A compliant constant-force mechanism for adaptive robot end-effector operations” *Proceedings - IEEE International Conference on Robotics and Automation* · June **2010**
- [4] Engin Tanık, Eres Söylemez, “Analysis and design of a compliant variable stroke mechanism”, pp 1385-1394 , *Mechanism and Machine Theory* , Elsevier, **2010**.
- [5] Howell, L. L., *Compliant Mechanisms*, John Wiley and Sons, New York, **2001**.
- [6] Jung-Yuan Wang , Chao-Chieh Lan, “A Constant-Force Compliant Gripper for Handling Objects of Various Sizes” , pp 7-9 *ASME*, July **2014**
- [7] Nathan, R. H., “A Constant Force Generation Mechanism,” *Journal of Mechanisms, Transmissions, and Automation in Design*, Trans. ASME, Vol. 107, December, pp. 508-512, **1985**.
- [8] Wahl, A., *Mechanical Springs*, 2nd. Ed. McGrawHill, New York, **1963**.
- [9] Yilin Liu and Qingsong Xu, “Design of a Compliant Constant Force Gripper Mechanism Based on Buckled Fixed-Guided Beam”, *IEEE*, **2016**.
- [10] M.D. Murphy, A. Midha, L.L. Howell, The topological synthesis of compliant mechanisms, *Mechanism and Machine Theory* 31 (1), 185–199 **1996**.
- [11] S.H. Brooks, S.P. Magleby, P. Halverson, L.L. Howell, Type synthesis of compliant 5-bar mechanisms with application to mechanical disc brakes, *Proceedings of the 13th National Conference on Mechanisms and Machines (NaCoMM07)*, Bangalore, India, , p. 103 **2007**.

[12] T. Laliberte, C. Gosselin, Simulation and design of underactuated mechanical hands, *Mechanism and Machine Theory* 33 (3) 39–57 **1998**.

[13] L.L. Howell, A. Midha, M.D. Murphy, Dimensional synthesis of compliant constant-force slider mechanisms, *Machine Elements and Machine Dynamics*, Vol. 71,, pp. 509–515, DE**1994**.

[14] B.D. Frischknecht, L.L. Howell, S.P. Magleby, Crank-slider with spring constant force mechanism, *Proceedings of the ASME Design Engineering Technical Conference 2A* , 809–817. **2004**.

[15] Engin Tanık Lecture Notes of MMU 634 ‘Rigid and Compliant Mechanism’, HacettepeUniversitesi, **2016**.

6 APPENDIXES

Appendix A – Matlab Code

Function;

```
function F = oguz(x)
Q13 = x(1); Q14 = x(2); S15 = x(3); T12 = x(4);

global a2 a3 a4 k34 k45 c

global Q12;

F = [linspace(80,-40,5) -40*ones(1,170) linspace(-40,200,10) 200*ones(1,170)
linspace(200,-40,10)];

f = F(ceil(Q12*180/pi)+1);

F(1) = cos(Q12) + (a3/a2)*cos(Q13) - (a4/a2)*cos(Q14) - S15/a2;

F(2) = sin(Q12) + (a3/a2)*sin(Q13) - (a4/a2)*sin(Q14);

F(3) = (Q13-Q14+c) * ( ( sin(Q12-Q13)/((a4/a2)*sin(Q14-Q13)) ) - (sin(Q12-
Q14)/((a3/a2)*sin(Q14-Q13))) ) ...
+ ((k45/k34)*(-Q14+c)*sin(Q12-Q13)/((a4/a2)*sin(Q14-Q13)) ) - T12/k34;

F(4) = (Q13-Q14+c) * ( (cos(Q13)/((a4/a2)*sin(Q14-Q13))) -
(cos(Q14)/((a3/a2)*sin(Q14-Q13)))) ...
+ (k45/k34)*(-Q14+c)*cos(Q13)/((a4/a2)*sin(Q14-Q13)) - (f*a2)/k34;
```

Run code;

```
clear; close all; clc;
global Q12;
fun = @oguz;
count = 1;

global a2 a3 a4 k34 k45 c
a2 = 1; a3 = 3; a4 = 1;
k34 = 100; k45 = 100; c = 2.618;

x0 = [0 0.1 1 1];
for Q12 = 0:pi/720:2*pi
    x = fsolve(fun,x0);
    X(count,:) = x;
    count = count + 1;
    x0 = x;
end

q12 = 0:pi/720:2*pi;

figure;
plot(q12*180/pi, radtodeg(X(:,1)));
hold on;
plot(q12*180/pi, radtodeg(X(:,2)));
xlabel('Q12[deg]'); ylabel(' [deg]');
legend('Q13', 'Q14');
```

```

ylim([-50 200]);grid on;

figure;
plot(q12*180/pi,X(:,3));
xlabel('Q12[deg]'),ylabel('S15[unit]');
ylim([1.5 5]);grid on;

figure;
plot(q12*180/pi,X(:,4));
xlabel('Q12[deg]'),ylabel('T12[Nunit]');
ylim([-250 50]);grid on;

```

For Design Chart

Function;

```

function F = oguz(x)
Q13 = x(1); Q14 = x(2); f = x(3); Q12 = x(4);
T12 = 0.5;
%S15 = x(3);
global a2 a3 a4 k34 k45 c S15

% global Q12;

% F = [linspace(80,-40,5) -40*ones(1,170) linspace(-40,200,10) 200*ones(1,170)
linspace(200,-40,10)];

% f = F(ceil(Q12*180/pi)+1);
% f=0;
F(1) = cos(Q12) + (a3/a2)*cos(Q13) - (a4/a2)*cos(Q14) - S15/a2;

F(2) = sin(Q12) + (a3/a2)*sin(Q13) - (a4/a2)*sin(Q14);

F(3) = (Q13-Q14+c) * ( ( sin(Q12-Q13)/((a4/a2)*sin(Q14-Q13)) ) - (sin(Q12-
Q14)/((a3/a2)*sin(Q14-Q13))) ) ...
+ ((k45/k34)*(-Q14+c)*sin(Q12-Q13)/((a4/a2)*sin(Q14-Q13)) ) - T12/k34;

F(4) = (Q13-Q14+c) * ( (cos(Q13)/((a4/a2)*sin(Q14-Q13))) -
(cos(Q14)/((a3/a2)*sin(Q14-Q13)))) ...
+ (k45/k34)*(-Q14+c)*cos(Q13)/((a4/a2)*sin(Q14-Q13))-(f*a2)/k34;

```

Run Code

```

clear; close all; clc;

fun = @oguz;
count = 1;

global a2 a3 a4 k34 k45 c S15
a2 = 100; a3 = 300; a4 = 60;
k34 = 2.5; k45 = 2.5; c = 2.618;

tS15 = linspace(252.1215,442.8*.8,20);
A4 = linspace(40,100,10);

```

```

x0 = [pi/8 120*pi/180 0 170*pi/180];

options = optimoptions('fsolve');
options = optimoptions(options,'Display','off');
options = optimoptions(options,'MaxFunEvals', 200000);
options = optimoptions(options,'MaxIter', 1000);
% fc = 0;
for fc=1:10
    a4 = A4(fc);
    for sc = 1:1:20
        S15 = tS15(sc);
        x = fsolve(fun,x0,options);
        X(count,:) = x;
        FF(fc,sc) = x(3);
        count = count + 1;
    %         x0 = x;
    end
end
XX = 442.8 - tS15
FF(4,:) * 1000
X(61:80,4) * 180/pi

q12 = 0:pi/720:2*pi;

```